Automotive Science and Engineering, Vol. 16, No. 2, (2026), 5042-5079

Iran University of Science and Technology

Automotive Science and Engineering

Journal Homepage: ase.iust.ac.ir

ISSN: 2008-9899

A Comprehensive Review on Hygrothermal Degradation of Adhesively Bonded Composite Joints: Nanoparticle Reinforcement Strategies and Cohesive Zone Modeling Approaches

Ali Keshavarzi, Hamed Saeidi Googarchin*[1]

Automotive Fluids and Structures Analysis Research Laboratory, School of Automotive Engineering, Iran University of Science and Technology, Tehran, Iran

ARTICLE INFO

Article history:

Received : 9 Dec 2025

Accepted: 27 Apr 2026

Published: 26 May 2026

Keywords:

Adhesive joints

Carbon Fiber Reinforced Polymers (CFRP)

Hygrothermal degradation

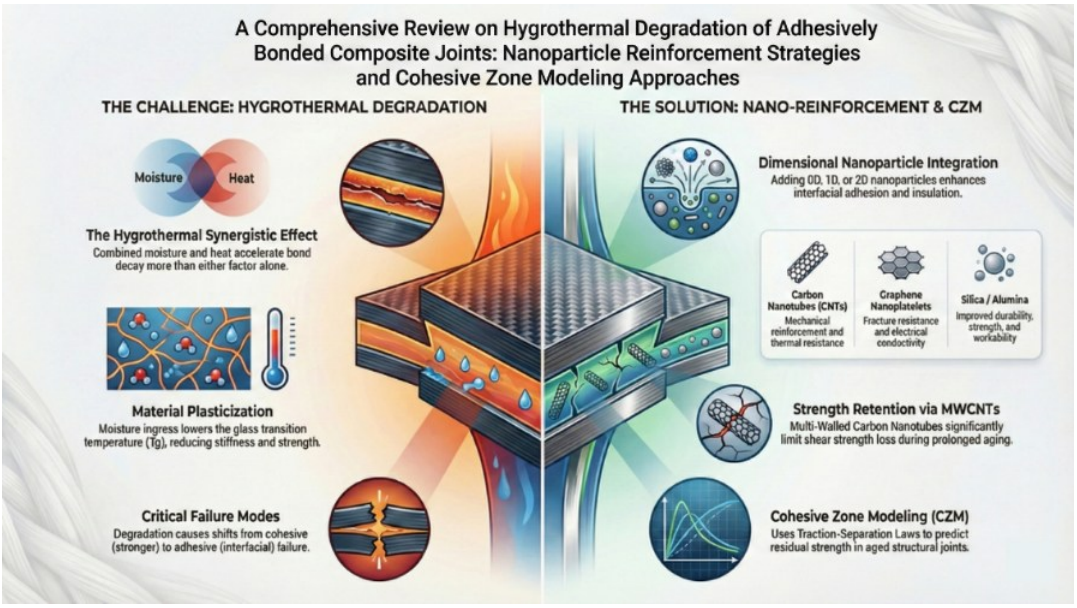
Nanoparticles

Cohesive Zone Model (CZM)

Automotive passive safety

A B S T R A C T

Adhesively bonded joints, particularly those featuring Carbon Fiber Reinforced Polymer (CFRP) adherends, have become indispensable in aerospace and automotive industries due to their superior strength-to-weight ratios. However, the long-term structural integrity of these joints is severely challenged by hygrothermal environments (the synergistic effect of moisture and temperature) which induces degradation in both the polymer matrix and the adhesive interface. This review provides a systematic discourse on the fundamental principles of composites, nanotechnology, and the mechanisms of environmental aging. It critically analyzes various joint configurations and failure modes, such as cohesive and adhesive failures, under adverse conditions. A significant portion of this study is dedicated to the efficacy of incorporating zero-, one-, and two-dimensional nanoparticles to enhance the environmental resilience of epoxy adhesives. Furthermore, this review evaluates the recent advancements in Cohesive Zone Modeling (CZM) for predicting the residual strength and fracture energy of aged joints through environment-dependent traction-separation laws. This work identifies critical gaps in accelerated aging methodologies and highlights the necessity for high-fidelity predictive models to ensure the safety of hybrid structures in high-stakes engineering applications.



*Corresponding Author
Email Address: hsaeidi@iust.ac.ir
https://doi.org/10.22068/ase.2026.741

"*Automotive Science and Engineering*" is licensed under a Creative Commons Attribution-Noncommercial 4.0 International License.

[Downloaded from rds.iust.ac.ir on 2026-11-19]

[DOI: 10.22068/ase.2026.741]

1. Introduction

Composites are engineered materials consisting of two or more constituent phases with distinct physical and chemical properties. Currently, among various composite categories, Polymer Matrix Composites (PMCs) have garnered significant attention across a wide spectrum of industries due to their exceptional strength-to-weight ratios, superior corrosion resistance, and design versatility [1]. Carbon Fiber Reinforced Polymers (CFRP), Glass Fiber Reinforced Polymers (GFRP), Aramid Fiber Reinforced Polymers (AFRP), and natural fiber-reinforced composites represent the most prevalent types of PMCs. The selection of a specific PMC is typically dictated by the required mechanical properties, cost considerations, and manufacturing constraints.

Compared to other PMCs, CFRP composites exhibit superior mechanical performance. These materials are predominantly joined using epoxy adhesives, which offer substantial benefits, including higher specific strength and enhanced fatigue life. Despite the widespread implementation of CFRP in the aerospace [2], automotive [3], and marine [4] industries, adhesive joints involving CFRP adherends are seldom utilized in primary load-bearing structures. This limitation stems from complex failure mechanisms that remain partially understood. This complexity is inherent to the integration of multiple materials with heterogeneous physical and mechanical characteristics. Furthermore, predicting their behavior is complicated by factors such as material anisotropy, size effects, non-linear material response, multi-modal failure, and environmental sensitivities [5, 6].

Among these factors, environmental stressors specifically humidity, temperature, and hygrothermal conditions (the synergistic effect of moisture and heat) can induce degradation in both the epoxy adhesive and the CFRP adherend. Such degradation ultimately compromises the long-term durability and structural integrity of the joint [7]. Consequently, recent research has focused on the incorporation of various nanoparticles into adhesives to enhance their mechanical properties and provide environmental insulation.

Therefore, the application of diverse laboratory techniques and advanced modeling frameworks is of paramount importance for the reliable prediction of degradation in nanoparticle-reinforced adhesive joints with composite adherends. These approaches are crucial for identifying potential failure mechanisms and developing robust strategies to mitigate joint failure [8]. Significant research efforts have been dedicated to achieving a more profound understanding of the fracture behavior of composite adhesive joints under hygrothermal exposure [9]. However, existing studies primarily rely on fracture experiments using conventional aging protocols, which are inherently time-consuming. This necessitates the adoption of accelerated aging methods, such as the open-face approach [10].

Nonetheless, significant challenges persist in integrating data derived from accelerated aging tests into the predictive failure models of real-scale joints. This review aims to address these critical gaps. As shown in Figure 1, to provide a comprehensive perspective, it is essential to first establish a foundation based on the existing literature, the fundamental principles of composites, and the vulnerability of adhesive bonds to hygrothermal environments. Accordingly, the subsequent sections provide a detailed discourse on the fundamentals of composites, adhesive bonding, and nanotechnology, followed by an in-depth analysis of the impacts of hygrothermal exposure on joint performance.

[Downloaded from rds.iust.ac.ir on 2026-11-19]

[DOI: 10.22068/ase.2026.741]

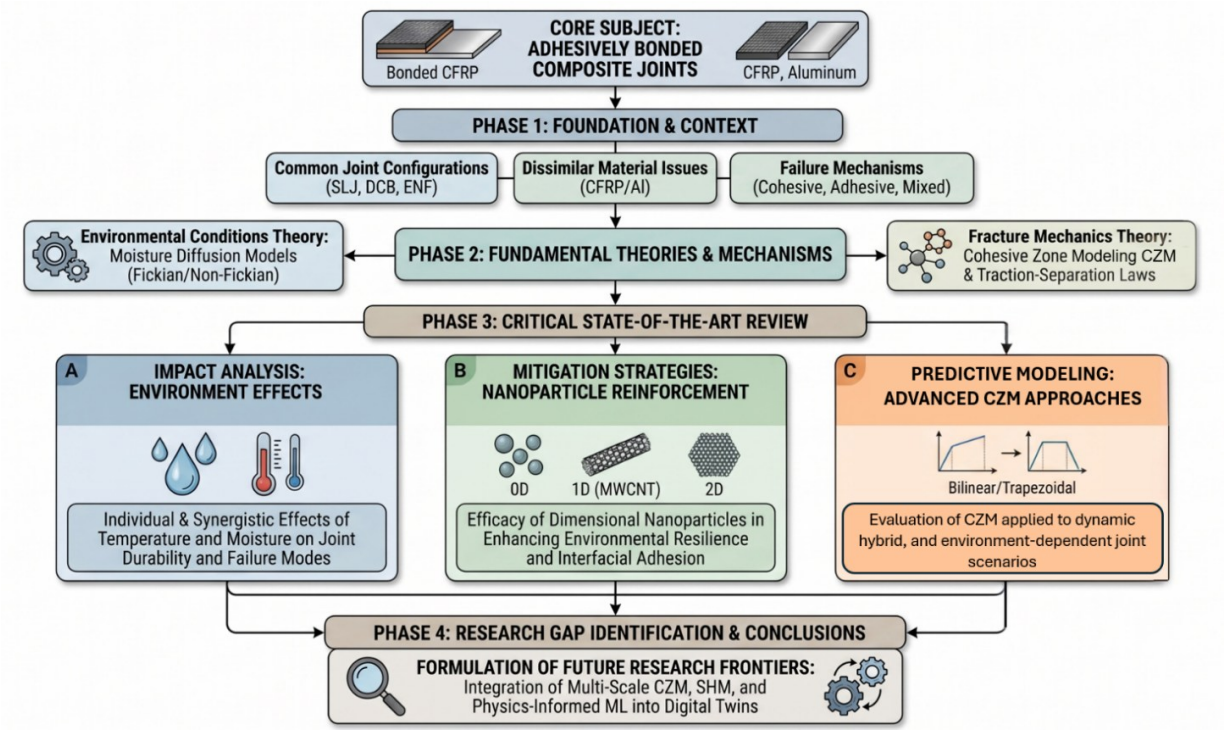


Figure 1 Schematic flowchart representing the organizational structure, key thematic areas, and methodology evaluated in this review.

2. Overview of Core Principles: Composites, Adhesive Bonding, and Nanotechnology

2.1. Composites

As illustrated in Figure 2, composites are engineered by combining several constituent materials with unique properties into a single structural entity. This integration results in a consolidated material possessing characteristics distinct from those of its individual components. Composites can be categorized through various methodologies; for instance, based on the type of reinforcement phase, they are classified into fiber-reinforced, particle-reinforced, and structural composites [1].

Following this classification, Fiber Reinforced Polymers (FRPs) are extensively employed across a diverse range of applications. Various types of FRPs are manufactured with different fiber orientations tailored to specific functional requirements. Depending on the end-use scenario, reinforcing fibers may be continuous, woven, chopped, or hybrid. Among these, continuous fibers offer the maximum directional reinforcement capability, which is frequently advantageous in advanced engineering disciplines.

Some of the most common continuous FRPs include CFRP, GFRP, and AFRP. In these systems, the fibers provide the primary load-bearing capacity and strength, while the matrix phase serves to support the fibers, protect them from environmental damage, and facilitate uniform load distribution among them.

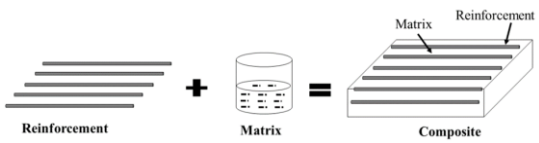


Figure 2 Schematic of FRPs

2.2. Adhesives

Adhesives are polymeric materials utilized to bond and resist the separation of two substances.

[Downloaded from rds.iust.ac.ir on 2026-11-19]

[DOI: 10.22068/ase.2026.741]

The term "adhesive" encompasses various materials such as cements, glues, and pastes, while the joined materials are typically referred to as adherends [11]. Adhesives are classified into various categories based on their physical, chemical, and bonding characteristics. Epoxy adhesives are a widely utilized and popular type of structural adhesive that offer several advantages. These adhesives consist of two parts resin and hardener which react to form a strong and durable bond. Their exceptional bonding properties make them suitable for joining various materials, including composites, plastics, and metals. Epoxy adhesives primarily consist of an epoxy resin, usually derived from di-glycidyl ether of bisphenol A [1], which undergoes a polymerization reaction [2] (step-growth or addition) with a curing agent containing amine, amide, or acid anhydride groups [3]. The curing agent reacts with the epoxy groups to form a thermoset polymer. This type of adhesive is widely used for bonding load-bearing structures in various industries and applications requiring durability and resistance to harsh environments.

2.3. Adhesives joints with composite adherends and automotive applications

The increasing number and variety of vehicles, coupled with rising operational speeds, have significantly contributed to the occurrence of traffic accidents, resulting in severe human injuries. Although vehicle designs and road infrastructures are continuously evolving, the complete eradication of road accidents remains an elusive goal. Currently, traffic collisions often cause severe or even fatal injuries to the individuals involved. Consequently, engineers specialized in passive safety have focused their efforts on mitigating the consequences of such accidents [12, 13].

Automotive passive safety systems incorporate energy-absorbing components designed to dissipate kinetic energy during crash scenarios. Structures engineered as energy absorbers must not only minimize the forces transmitted to the vehicle's occupants but also possess the capability to reduce the impact forces on pedestrians and individuals outside the vehicle. Therefore, the design of structures capable of irreversible energy absorption without detrimental environmental impacts is of paramount importance [14]. Figure 3 illustrates the evolutionary trends in designing a bio-inspired geometry for energy absorbers.

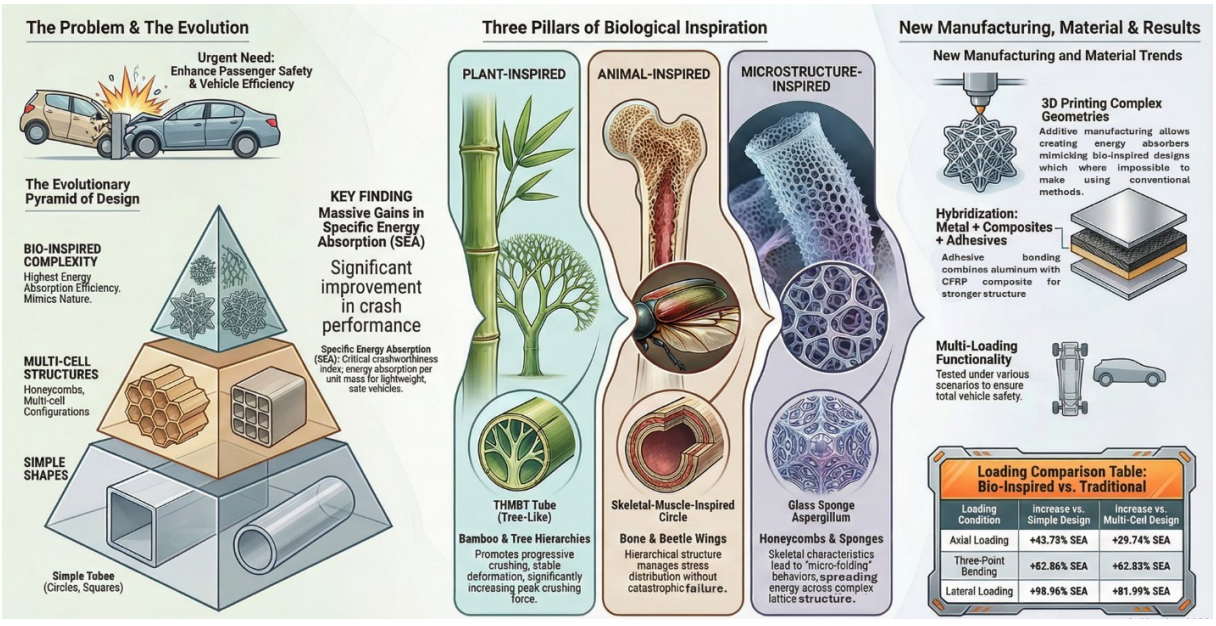


Figure 3 The evolutionary trends in bio-inspired energy absorbers [14].

[Downloaded from rds.iust.ac.ir on 2026-11-19]

[DOI: 10.22068/ase.2026.741]

As previously noted, adhesive joints featuring composite adherends are extensively utilized across various sectors, including aerospace, automotive, marine, and wind energy industries, due to their superior strength-to-weight ratios and exceptional durability [15]. Specific applications of CFRP-based composites and their corresponding adhesive joints are depicted in Figure 4 [16, 17].

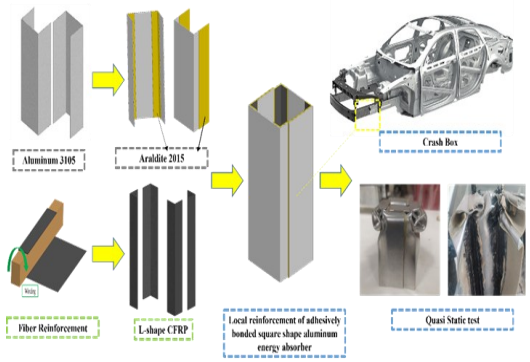


Figure 4 Common type of application of adhesive, composite, and metal joints together [16, 17].

2.4. Joint Configurations and Failure Mechanisms

Various adhesive joint configurations are implemented in engineering practice, including butt joints, single and double lap joints, and stepped lap joints, as illustrated in Figure 5. The selection of a specific joint design is critically influenced by factors such as the adhesive type, the properties of the adherends, the anticipated stress levels, and the required structural strength. The most prevalent configurations are discussed below [11]:

• Butt Joint: A configuration in which two members are joined at a 90-degree angle. This joint is commonly utilized in structural frames and is capable of resisting both tensile and compressive loads.

• Single Lap Joint (SLJ): In this configuration, one adherend surface overlaps another. SLJs are predominantly used in applications where the joint is subjected to shear loading.

• Strap Lap Joint: This involves adding a strap or reinforcement to a single lap joint to enhance its load-bearing capacity. This design is widely adopted in scenarios where the joint is exposed to extreme stress conditions.

• Double Lap Joint (DLJ): A configuration where both surfaces of the adherends overlap. Compared to single lap joints, DLJs provide significantly higher strength and enhanced long-term durability.

• Stepped Lap Joint: This features a stepped overlap between the adherends. This configuration is typically preferred when an exceptionally robust and high-performance bond is required.

Figure 5 presents these various joint types along with representative examples of their industrial applications.

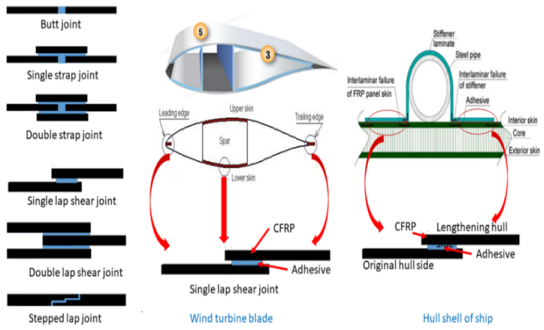


Figure 5 Types of joints and connections in common applications [18].

Among the various joint configurations previously discussed, Single Lap Joints (SLJs) are the most extensively utilized in structural applications. Figure 5 illustrates their implementation in demanding sectors such as wind turbines and marine engineering.

Since these joints are frequently subjected to diverse environmental stressors for extended durations, their physical and mechanical properties are susceptible to significant degradation or alteration resulting from such exposure.

The factors governing the failure modes of adhesive joints encompass surface preparation conditions, material parameters, geometric configurations, and environmental variables [19]. The intricate interplay between these factors and their subsequent impact on various failure

[Downloaded from rds.iust.ac.ir on 2026-11-19]

[DOI: 10.22068/ase.2026.741]

mechanisms introduces a high level of complexity, making the development of accurate predictive models a formidable challenge. Figure 6 depicts several predominant failure modes observed in adhesive joints.

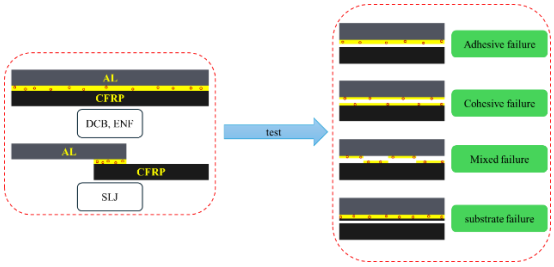


Figure 6 Typical failure modes in FRP composite adhesive bonding [20].

2.5. Advantages, Disadvantages, and Limitations of Adhesive Joints

Adhesive joining offers several notable benefits, including considerable static and fatigue strength, effective sealing performance, and strong capability for vibration attenuation. In addition, because loads are transmitted more evenly throughout the bonded interface, local stress concentrations are reduced, which can improve the fatigue durability of the connection. Another important benefit is that this technique avoids the need for mechanical fastening processes such as drilling, thereby preventing damage to the joined substrates. Adhesive bonding also contributes to structural weight reduction; however, one of its most significant merits is its suitability for joining dissimilar materials [9]. This feature makes it particularly attractive for incorporating modern lightweight materials, including composites, into vehicle structures as part of weight-saving strategies.

Despite these advantages, adhesive joints are associated with several challenges. In particular, their mechanical performance is highly sensitive to service environment parameters such as temperature and moisture exposure. Variations in these conditions may degrade the bond strength and, in severe cases, result in sudden joint failure. The principal drawbacks of adhesive bonding include:

- Requirement for precise and rigorous design.
- Difficulty in long-term life estimation and durability prediction.
- Necessity for meticulous surface preparation.
- Need for specialized fixtures and clamping during the bonding process.
- Requirement for controlled curing cycles.
- Sensitivity to environmental degradants.
- Vulnerability to peeling and cleavage stresses.
- Presence of residual stresses induced during the curing process.

2.6. Degradation in Adhesive Joints

An adhesive joint is considered to have undergone degradation when it experiences changes in its physical properties, such as mechanical strength, relative to its initial state. Since adhesive joints are frequently exposed to diverse environmental conditions, the impact of such variables must be integrated into any comprehensive study. Temperature, moisture, and UV exposure duration are the most prevalent environmental variables [11], with temperature and moisture being the primary drivers of degradation.

The term hygrothermal refers to the synergistic effect of these two factors. Nevertheless, accurately predicting the degradation of adhesive joints in response to environmental stressors remains a complex task. This complexity arises from a limited understanding of the underlying degradation mechanisms, the lack of standardized and reliable testing methodologies, and the inherently time-consuming nature of aging experiments [11].

2.7. Introduction to Nanoparticles and Their Role in Adhesive Reinforcement

Materials can be classified based on their structure, properties, applications, and dimensions. A particularly significant classification is the categorization of nanomaterials based on their dimensionality. This section provides a brief overview of various nanostructures and discusses their fundamental differences [21].

[Downloaded from rds.iust.ac.ir on 2026-11-19]

[DOI: 10.22068/ase.2026.741]

2.7.1. Introduction to Nanostructures

All materials occupy a three-dimensional framework composed of length, width, and height. A material is generally regarded as a nanostructure when at least one of these dimensions lies within the nanometer scale. Although no single definition of nanomaterials has been universally standardized, the description proposed by the U.S. National Nanotechnology Initiative (NNI) is among the most commonly adopted. Based on this definition, nanomaterials are materials whose characteristic dimensions are smaller than 100 nm. Nevertheless, in some studies, materials with dimensions slightly above this threshold are also considered within the scope of nanomaterials [21].

The nanoscale corresponds to a dimensional regime in which materials exhibit properties markedly different from those observed in their bulk form. One of the most frequently used approaches for classifying nanomaterials is to consider how many of their dimensions are within the nanometer range. As shown in Figure 7, nanomaterials can therefore be divided into three main categories:

- Zero-dimensional (0D) nanostructures: Materials where all three dimensions are at the nanoscale.
- One-dimensional (1D) nanostructures: Materials where two dimensions are at the nanoscale.
- Two-dimensional (2D) nanostructures: Materials where only one dimension is at the nanoscale.

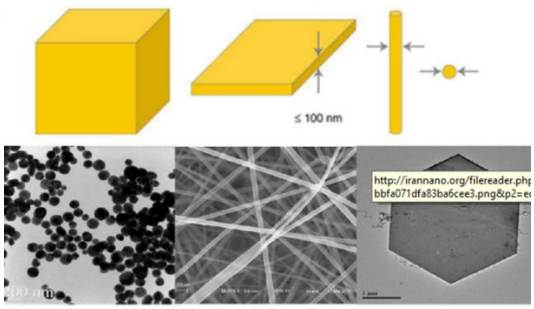


Figure 7 A schematic of types of zero-, one-, and two-dimensional nanomaterials along with images taken with electron microscopes [21].

The dimensional classification of nanomaterials is regarded as one of the most critical taxonomies in the field. These three categories of nanostructures exhibit profound differences concerning their synthesis methodologies, production techniques, physicochemical properties, and practical applications. Their electrical, optical, magnetic, and surface characteristics vary substantially, which consequently dictates their specialized and unique industrial and scientific utilities.

For instance, zero- (0D), one- (1D), and two-dimensional (2D) nanomaterials demonstrate distinct capacities for light absorption and emission. Specifically, 1D nanostructures are uniquely suited for electronic interconnects, an application for which 0D and 2D nanomaterials are generally unsuitable. A critical nuance in this dimensional classification is that for 1D nanomaterials, it is not strictly required that only one dimension resides outside the nanoscale; rather, 1D materials can be synthesized with all three dimensions within the nano-range, provided that one dimension is significantly (several orders of magnitude) larger than the other two. Similarly, in the case of 2D nanomaterials, while dimensions may fall within the nanoscale, two of these dimensions must be substantially larger than the third [21]. Figure 8 presents images of 1D and 2D nanostructures captured via Transmission Electron Microscopy (TEM).

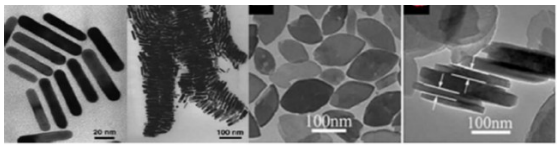


Figure 8 images of one-dimensional and two-dimensional nanostructures taken with a transmission electron microscope [21].

Zero-dimensional (0D) nanomaterials represent one of the most significant classes of nanoscale structures. In comparison with one-dimensional and two-dimensional nanomaterials, their

[Downloaded from rds.iust.ac.ir on 2026-11-19]

[DOI: 10.22068/ase.2026.741]

broader acceptance and more extensive utilization are largely associated with easier fabrication methods and reduced manufacturing expenses. Typical examples of 0D nanomaterials include fullerenes, quantum dots, and nanoclusters [21].

One-dimensional (1D) nanostructures can generally be categorized as nanorods, nanowires, or nanotubes. This classification is based on features such as the geometry of the cross section and the aspect ratio, which is defined as the proportion of length to cross-sectional diameter. After preparation, these nanomaterials are commonly either suspended in a surrounding medium, most often a solvent, or grown in a vertically aligned arrangement on a solid support or template. Among the best-known representatives of 1D nanostructures are quantum wires and carbon nanotubes [21].

Two-dimensional (2D) nanostructures are typically classified into thin films, nanosheets, and nanoplates. Well-established examples of this group include graphene and quantum wells, both of which have attracted considerable attention because of their unique structural and functional characteristics.

As summarized in Table 1, nanoparticles with different compositions and formulations can play an important role in improving material performance and strengthening adhesive joints. The addition of nanoparticles to adhesive systems helps address several inherent shortcomings while enhancing key properties, including tensile strength, adhesion capability, and fracture resistance. Owing to their extremely small dimensions and large specific surface area, nanoparticles can interact efficiently with the adhesive matrix and act as reinforcing agents within the structure. Their presence also promotes a more homogeneous transfer of mechanical stress and improves interfacial bonding in different regions. In addition, certain nanoparticles, particularly metallic and oxide-based types, can increase resistance to thermal exposure, humidity, and corrosive environments, which ultimately leads to longer service life and greater durability of adhesive joints.

Table 1 Common nanoparticles and their functions in epoxy adhesives.

Nanoparticle Category	Specific Type	Characteristics/Functions	Reference
Carbon-based	Nano-diamond	Tribological properties	[22-25]
	Carbon Nanotubes (CNTs)	Mechanical and thermal reinforcement, electrical conductivity	[26-28]
	Carbon Nanofibers (CNFs)	Thermal resistance, mechanical reinforcement	[29, 30]
	Graphene Nanoplatelets (GNPs)	Electrical conductivity, lubrication, fracture resistance	[31, 32]
	Graphene Oxide (GO) Nanoplatelets	Flame retardancy	[33-35]
Inorganic	Clay Nanosheets	Low cost, flame retardant, rheological modifier, mechanical reinforcement, liquid penetration resistance	[36, 37]
	Halloysite Nanotubes (HNTs)	Low cost, toughening agent, mechanical reinforcement	[38, 39]
	Gold Nanoparticles	Tunable optical and electronic properties	[40]

[Downloaded from rds.iust.ac.ir on 2026-11-19]

[DOI: 10.22068/ase.2026.741]

Metal/Metal-Oxide based	Silver Nanoparticles	Antibacterial properties, electrical conductivity	[41]
	Al_2O_3	Mechanical and thermal reinforcement, wear resistance, electrical properties, adhesion	[42, 43]
	ZrO_2	Electrical properties, arc resistance	[44, 45]
	Fe_3O_4	Magnetic properties	[46, 47]
Silica	Nano-silica	Improvement of strength, flexibility, durability, and workability	[48, 49]
Rubber	Rubber Nanoparticles	Toughening agent	[50]

2.8. Summary of Section 2

This section has highlighted the critical importance of composite materials, specifically Polymer Matrix Composites (PMCs), and the growing adoption of adhesive bonding as a preferred joining technique across various sectors, most notably the automotive industry. It has further emphasized the necessity of understanding and managing environmental degradation in adhesive joints. This issue remains a formidable challenge that restricts the broader implementation of adhesively bonded composite structures.

Furthermore, the preceding discussion underscored the imperative for high-fidelity predictive models capable of accounting for the synergistic effects of environmental factors, such as humidity and temperature, on joint performance. Such models are essential for the design and realization of safe, durable, adhesively bonded composite structures in high-stakes industries like automotive engineering.

Ultimately, this section serves as the foundational framework for the proposed research. This study aims to address the challenges posed by environmental degradation in composite/metal hybrid structures. This objective is pursued through the synthesis and incorporation of specialized nanoparticles into the adhesive to enhance its environmental resistance, coupled with the development of a Cohesive Zone Model (CZM) that accurately predicts joint behavior under varying hygrothermal conditions. The following section provides a comprehensive review of prior literature to offer a deeper understanding of existing research and to identify potential avenues for further investigation.

3. Fundamentals, Procedures, and Governing Theories

This section introduces the procedures, mechanisms, and governing theories pertinent to the research problem addressed in this review article. In this regard, the effects of moisture are examined first, followed by the impact of adherend dissimilarity. Finally, the mechanics and governing theories of the Cohesive Zone Model (CZM) and the Traction-Separation Law (TSL) are discussed.

3.1. Fundamentals of the Cohesive Zone Model

The Cohesive Zone Model in fracture mechanics, developed based on the foundational studies of Dugdale [51] and Barenblatt [52], is recognized as a highly efficient computational method for simulating damage evolution. This model investigates crack propagation in materials and postulates that when a pre-cracked material is subjected to loading, microcracks begin to initiate within a localized region known as the Fracture Process Zone (FPZ).

Within this zone, the stress at the crack tip increases as the separation between the surfaces increases. Upon reaching a critical stress

[Downloaded from rds.iust.ac.ir on 2026-11-19]

[DOI: 10.22068/ase.2026.741]

threshold, T_0, this stress gradually softens and decreases until it completely diminishes to zero. At this exact moment, new fracture surfaces are generated, and the macroscopic crack propagates through the material. This variation of applied stress relative to the crack opening displacement is graphically represented by a traction-separation curve, widely known as the "Traction-Separation Law" [53].

According to this model, the underlying structural micromechanisms can be entirely described by two fundamental cohesive variables:

- Damage Initiation Stress (T_0): The critical stress at which the separation of surfaces initiates.
- Separation Limit (δ_0): The ultimate separation value beyond which the cohesive element completely loses its load-bearing capacity, leading to crack propagation by one element length.

Furthermore, as illustrated in Figure 9, the integral under the traction-separation curve, which equates to the fracture energy G_I or G_{II}, can also serve as an alternative parameter to characterize fracture behavior (this cohesive element is depicted in Figure 10). This energetic approach facilitates a more comprehensive description of material behavior under fracture and crack propagation conditions.

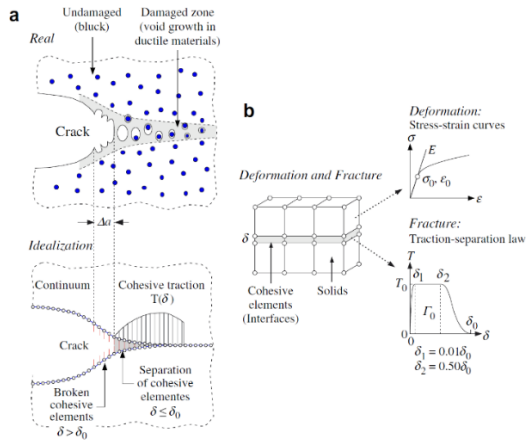


Figure 9 Cohesive Zone Model: (a) Schematic of the physical process of separation and crack growth and its modeling; (b) Application of cohesive elements to connect material elements and the corresponding traction-separation diagram [53].

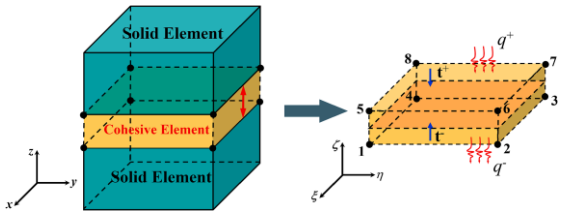


Figure 10 8-node zero-thickness cohesive element [54].

3.1.2. Fundamentals and Theory of the Traction-Separation Law

To directly extract the parameters of the cohesive zone model, two principal approaches can be employed:

- Linear Elastic Fracture Mechanics (LEFM): This approach is utilized to analyze the fracture behavior of materials under the assumption of linear elasticity. The objective of employing LEFM is to derive a relationship between the adhesive fracture energy in Mode I or Mode II and the crack opening displacement. This relationship is obtained by curve-fitting the data extracted from Digital Image Correlation (DIC) recorded during experimental testing.
- J-Integral Theory: This approach, which is particularly highly applicable in the analysis of cohesive materials and complex fracture phenomena, calculates the fracture energy utilizing the J-integral. This theory allows for a more rigorous and precise investigation of stress distributions and fracture energies within the cohesive zone.

To evaluate the fracture state under mixed-mode loading, the fracture energies associated with the pure modes (Mode I and Mode II) are required. Prevailing research indicates that the fracture energy in Mode II and Mode III are typically

[Downloaded from rds.iust.ac.ir on 2026-11-19]

[DOI: 10.22068/ase.2026.741]

assumed to be equal [55]. This assumption is justified by the similarities in the underlying fracture mechanisms of these shear modes and facilitates analytical simplification.

Consequently, for accurate analysis and derivation of cohesive zone parameters, data obtained from digital images can be coupled with appropriate curve-fitting techniques based on either LEFM or the J-integral theory.

3.1.3. Fundamentals and Theory of the Classic Bilinear Model

As previously stated, various phenomenological models have been proposed to describe the traction-separation law. In the present proposal, the bilinear model has been selected as the definitive choice. The bilinear traction-separation model demonstrates robust accuracy in evaluating the behavior of the adhesive layer. To model the linear elastic behavior of the adhesive prior to damage initiation, the following constitutive relationship is established:

$$\begin{bmatrix}\sigma_n\\ \sigma_s\\ \sigma_t\end{bmatrix}=\begin{bmatrix}K_{nn} & 0 & 0\\ 0 & K_{ss} & 0\\ 0 & 0 & K_{ff}\end{bmatrix}\begin{bmatrix}\delta_n\\ \delta_s\\ \delta_t\end{bmatrix} \quad (1)$$

Where σ is the stress matrix, δ is the crack opening separation matrix, and K represents the initial stiffness matrix.

According to Figure 11, the bilinear model initially assumes a linear elastic response, followed by damage initiation and subsequent damage evolution. The crack opening displacement at the onset of damage and the final failure separation are calculated based on the following relations:

$$\delta_i^0=\frac{\sigma_i}{k_{ii}}, i=n,s,t \quad (2)$$

$$\delta_i^f=\frac{2G_{IC/IIC}}{\tau_{ic}}, i=n,s,t \quad (3)$$

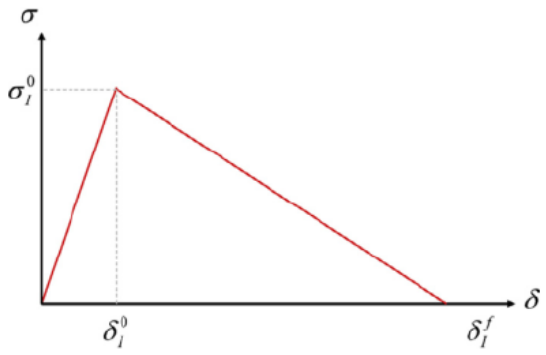


Figure 11 Bilinear Traction-Separation Model

Damage initiation is governed by various criteria, generally categorized into two main groups: stress-based criteria and strain-based criteria. Stress-based criteria encompass the maximum nominal stress (MAXS) and quadratic nominal stress (QUADS), whereas strain-based criteria include the maximum nominal strain (MAXE) and quadratic nominal strain (QUADE). The mathematical formulations for these criteria are summarized in Table 2 [56].

Table 2 Damage Initiation Criteria [56].

Stress Based	Strain Based
$MAXS: \max\left\{\frac{\langle\sigma_n\rangle}{\sigma_n^0}, \frac{\sigma_s}{\sigma_s^0}\right\}$	$MAXE: \max\left\{\frac{\langle\varepsilon_n\rangle}{\varepsilon_n^0}, \frac{\varepsilon_s}{\varepsilon_s^0}\right\}$
$QUADS: \left\{\frac{\langle\sigma_n\rangle}{\sigma_n^0}\right\}^2+\left\{\frac{\sigma_s}{\sigma_s^0}\right\}^2=1$	$QUADE: \left\{\frac{\langle\varepsilon_n\rangle}{\varepsilon_n^0}\right\}^2+\left\{\frac{\varepsilon_s}{\varepsilon_s^0}\right\}^2=1$

**ε_s and ε_n are the instantaneous strains, ε_s^0 and ε_n^0 are the ultimate strains, and the Macaulay brackets < > are used to signify that compressive stresses do not initiate damage.*

Total separation and complete failure are dictated by a damage evolution criterion. Based on the power law criterion, failure is determined using a relationship where the equivalent mixed-mode energy equals the energy required to induce failure in pure Modes I and II. Additionally, the Benzeggagh-Kenane (BK) criterion is an efficient and widely adopted approach, especially since fracture behaviors in Modes II and III are treated identically.

[Downloaded from rds.iust.ac.ir on 2026-11-19]

[DOI: 10.22068/ase.2026.741]

$$Power-Law:\left\{\frac{G_I}{G_{Ic}}\right\}^2+\left\{\frac{G_{II}}{G_{IIc}}\right\}^2=1 \quad (4)$$

$$BK: G_{Ic}+(G_{IIC}+G_{IC})\left\{\frac{G_{II}+G_{III}}{G_I+G_{II}+G_{III}}\right\}^{\eta}=G_C \quad (5)$$

Where η is the mode-mixity ratio and acts as a material constant.

In a 2018 study, Rocha and Campilho [57] investigated Araldite 2015 adhesive and found that both stress-based damage initiation criteria yield results that closely align with experimental data. The percentage of deviation for these two criteria compared to experimental results for an overlap length of 50 mm was 8.8% for MAXS and 0.8% for QUADS. Upon reducing the overlap length to 25 mm, this deviation decreased to 7.3%. The findings also demonstrated that strain-based criteria were unsuitable for this specific adhesive, exhibiting significant discrepancies with experimental observations. Based on these findings, the QUADS criterion for damage initiation and the power law (or BK) criterion for damage evolution have been identified as the most appropriate choices.

3.1.4. Pure Mode I in Dissimilar Specimens

One of the fundamental challenges in the study of dissimilar (bi-material) joints is the methodology for extracting the precise properties of the specimen under pure Mode I loading. Currently, standardized test methods for fracture energy extraction are exclusively established for similar (homogeneous) specimens, and no universal standard test exists for dissimilar configurations.

A comprehensive review of the literature suggests that flexural stiffness matching (bending stiffness equalization) of the two adherends is the most widely adopted design criterion for dissimilar specimens. This approach ensures that under identical loading conditions, both adherends deform uniformly, thereby making the subsequent analytical interpretation more straightforward and reliable [58].

As depicted in the schematic of the crack opening displacement in Figure 12, kinematic relations indicate that in addition to Mode I (vertical crack opening), Mode II (interfacial shear sliding of the crack faces) can also be induced, as detailed below. This highlights the inherent complexity in the analysis and design of dissimilar joints, where mixed-mode fracture conditions are highly prone to occur.

Accounting for this phenomenon in the experimental design and numerical modeling of composite material fracture behavior is critically important, as a rigorous understanding of fracture micromechanisms can significantly contribute to the optimization of materials and joining methodologies.

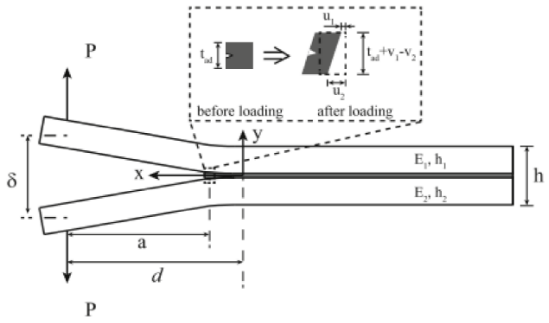


Figure 12 schematic of deformation near the adhesive crack tip in a DCB specimen [58].

$$\varepsilon_{yy}=\frac{v_1-v_2}{t_{adhesive}} \quad (6)$$

$$\gamma_{yy}=\frac{u_1-u_2}{t_{adhesive}} \quad (7)$$

Where E_1 and E_2 are the elastic moduli, h_1 and h_2 are the thicknesses of the adherends, a is the crack length, d is the distance from the applied load to the neutral axis, ε_{yy} is the normal strain, and γ_{yy} is the shear strain. Assuming negligible shear strain, the expression reduces to:

$$u_1=u_2 \quad (8)$$

[Downloaded from rds.iust.ac.ir on 2026-11-19]

[DOI: 10.22068/ase.2026.741]

Consequently, the following condition must be satisfied:

$$E_1 h_1^2 = E_2 h_2^2 \quad (9)$$

To achieve identical bending in both adherends, their flexural stiffness must be equal:

$$E_1 h_1^3 = E_2 h_2^3 \quad (10)$$

Evidently, if both adherends are identical, pure Mode I is readily attainable, as both materials respond symmetrically to the applied load. However, if the adherends differ (dissimilar joint), the experimental setup must be designed according to specific criteria.

The two predominant criteria for designing dissimilar joints are [58]:

1. Strain-based criterion (Equation 9): This design criterion is implemented when the objective is to equalize the strain distribution along the joint overlap.
2. Bending-based criterion (Equation 10): This criterion is applied when the goal is to equalize the bending moment distribution across the two arms of the specimen.

In certain studies [59], to mitigate this complexity, composite adherends have been tailored such that their ultimate elastic modulus and thickness are as close as possible (or practically equal) to those of the metallic adherend. Due to the inherent discrepancies in the mechanical and structural properties of dissimilar materials, this approach remains highly challenging.

For composite/metal Double Cantilever Beam (DCB) specimens, research has demonstrated that utilizing the strain-based criterion yields higher precision in results [58]. Nevertheless, the application of simplified reduced equations relies strictly on the condition that the flexural characteristics of both specimen arms are identical.

Therefore, in this proposal, the bending-based criterion is adopted. This selection is driven by the necessity for enhanced analytical precision and the need to rigorously account for the complexities arising from multi-material structural assemblies.

3.2. Hygrothermal Conditions

This section investigates the theoretical fundamentals and governing constitutive equations related to moisture absorption and hygrothermal conditioning in structural adhesives. As previously mentioned, hygrothermal conditions refer to the synergistic combination of moisture and temperature, which can significantly degrade the mechanical and chemical integrity of adhesives. Comprehending these environmental conditions and the corresponding material response is absolutely vital for the structural design and optimization of adhesively bonded joints operating in such harsh environments.

3.2.1. Fundamentals and Theory of Moisture Diffusion

According to the foundational investigations by Hopfenberg and Frisch [60], various diffusion processes can occur during the penetration of a solute into a solvent. A summary of these specific diffusion conditions is detailed below:

- Concentration-independent Fickian diffusion: Occurs when the rate of polymer relaxation in the adhesive is significantly lower than the mobility of the water molecules. This type of diffusion predominantly takes place at temperatures well below the glass transition temperature (T_g). During the diffusion process, the concentration gradient continuously diminishes until it reaches equilibrium (zero).
- Concentration-dependent Fickian diffusion: Occurs when polymer relaxation in the adhesive is a time-dependent function. This mechanism typically manifests at temperatures above

[Downloaded from rds.iust.ac.ir on 2026-11-19]

[DOI: 10.22068/ase.2026.741]

the glass transition temperature (T_g). Consequently, the diffusion becomes boundary-concentration-dependent and time-dependent.

- Non-Fickian or Anomalous diffusion: Arises when the mobility of the water molecules and the polymer relaxation rate are comparable. This usually occurs at temperatures below T_g and is frequently correlated with the crystalline regions of the polymer network.
- Case II diffusion: Happens when the mobility of the permeating water molecules is drastically higher than the polymer relaxation rate. This occurs at temperatures below T_g and induces severe internal swelling stresses.
- Crazing: Generally recognized as a subset of Case II diffusion. It occurs when the mobility of water molecules is exceptionally high and is usually the consequence of anomalous diffusion occurring in localized regions.

The penetration of water molecules induces plasticization, which inherently involves the dilation of intermolecular free volume to accommodate further absorption, thereby increasing the segmental mobility of the adhesive's polymeric chains and consequently deteriorating its ultimate macroscopic strength.

To mathematically model the moisture diffusion into the adhesive, Fick's diffusion model is employed, which adequately characterizes the water absorption behavior of adhesives at temperatures below the glass transition temperature. According to this model, the diffusion flux, J, is proportional to the concentration gradient $d\varphi/dx$ and the diffusion coefficient D:

$$J = -D\nabla\varphi\frac{d\varphi}{dx} \tag{11}$$

$$\frac{d\varphi}{dt} = D\nabla^2\varphi \tag{12}$$

Assuming that the thickness of the adhesive layer is infinitesimally small compared to its planar dimensions, the diffusion equations can be simplified and rewritten in one-dimensional form:

$$J = -D\frac{d\varphi}{dx} \tag{13}$$

$$\frac{d\varphi}{dt} = D\frac{\partial^2\varphi}{\partial x^2} \tag{14}$$

The analytical solution to the one-dimensional Fickian diffusion equation is expressed as follows:

$$\frac{\varphi(x,t)}{\varphi_\infty} = 1 - \frac{4}{\pi}\sum_0^\infty \frac{(-1)^n}{2n+1}\left[e^{\left(-\frac{D(2n+1)^2\pi^2 t}{ah^2}\right)}\cos\frac{(2n+1)nx}{2h}\right] \tag{15}$$

Where φ_∞ represents the equilibrium concentration at the boundaries and t is the elapsed time. The diffusion coefficient can be experimentally extracted using the following relationship:

$$D = \pi\left(\frac{h}{4M_\infty}\right)^2\left(\frac{M_2 - M_1}{\sqrt{t_2} - \sqrt{t_1}}\right)^2 \tag{16}$$

Where h is the specimen thickness, and M_1 and M_2 are the fractional moisture uptakes at times t_1 and t_2, respectively.

The fractional moisture uptake, M_t, defined as the ratio of the total mass of absorbed moisture at time t to the initial mass of the dry specimen (expressed as a percentage), is calculated as:

$$\frac{M_t}{M_\infty} = 1 - \frac{8}{\pi^2}\sum_0^\infty \frac{(-1)^n}{(2n+10)^2}\left[e^{\left(\frac{-D(2n+1)^2\pi^2 t}{4h^2}\right)}\right] \tag{17}$$

Where M_∞ is the saturation (equilibrium) weight gain.

[Downloaded from rds.iust.ac.ir on 2026-11-19]

[DOI: 10.22068/ase.2026.741]

The determination of the fractional weight gain, M_t, is conducted via gravimetric measurements, and its numerical value is given by Equation 18:

$$M_t = \frac{w_t - w_i}{w_i} \times 100\% \quad (18)$$

3.2.2. Procedure for Applying Temperature and Moisture to Laboratory Specimens

The conventional methodology for conditioning laboratory specimens under varying temperature and humidity profiles involves placing them inside controlled environmental humidity chambers. As depicted in Figure 13, over extended periods, moisture permeates from the exposed boundaries into the core of the specimen.

In this configuration, the diffusion process is extremely sluggish due to the extended diffusion path length, and it may require several months for uniform saturation to occur. Furthermore, mechanical testing results obtained prior to complete saturation cannot be reliably extrapolated to other specimens due to the severe non-uniformity of the moisture concentration gradient [61]. To circumvent this critical limitation, Chang [62] proposed that diffusion uniformity must be optimized. Additionally, to mitigate galvanic or environmental corrosion, the application of primer coatings rather than mechanical machining is highly recommended to prevent the initiation of surface microcracks.

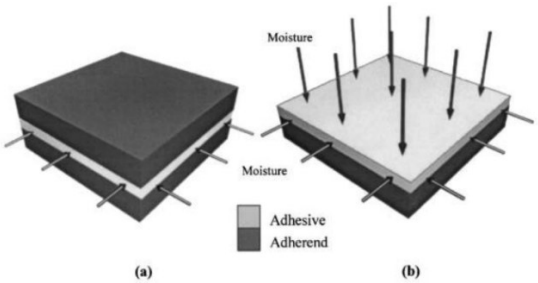


Figure 13 Moisture application methods. Left: Conventional method; Right: Open-faced method [61].

To drastically accelerate the moisture absorption kinetics and concurrently ensure a homogeneous moisture distribution, "open-faced" specimens can be utilized, as illustrated in Figure 14. In this approach, the individual adherends are conditioned prior to bonding. Following saturation, the adherends are removed from the environmental chamber, their surfaces are meticulously wiped dry, and they are immediately bonded together using the structural adhesive.

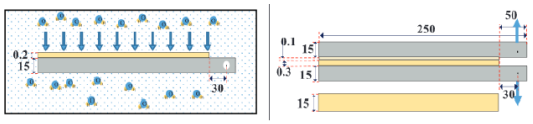


Figure 14 Preparation process of open-faced specimens [15].

3.2.3. Environmental Degradation of Adhesive Joints with Composite Adherends

The majority of investigations focusing on the prediction of degradation behavior under various environmental exposures heavily rely on analytical, computational, and experimental methodologies. For instance, Phani and Bose [63] proposed a semi-empirical model elucidating how intrinsic material properties degrade under hygrothermal conditions. This continuous degradation model successfully predicts strength retention in wet environments, where the residual strength after an exposure time t is given by Equation 19:

$$\sigma(t) = (\sigma_0 - \sigma_\infty) \times e^{mt} + \sigma_\infty \quad (19)$$

Where σ_0 denotes the initial strength of the unconditioned joint, σ_∞ denotes the residual strength after prolonged (infinite) exposure to the specific environmental conditions, and m represents the rate of degradation. The degradation rate m can be evaluated using the

[Downloaded from rds.iust.ac.ir on 2026-11-19]

[DOI: 10.22068/ase.2026.741]

Arrhenius equation, as formulated in Equation 20 [64]:

$$m = B \times e^{(-\frac{Ed}{RT})} \quad (20)$$

Where B is a material-dependent pre-exponential constant, Ed represents the activation energy for degradation, R is the universal gas constant, and T denotes the absolute temperature. The Arrhenius expression can similarly be adapted to compute the activation energy governing water diffusion, defined by Equation 21 [64]:

$$D = D_0 \times e^{(-\frac{Ed}{RT})} \quad (21)$$

Where D_0 is the pre-exponential diffusion constant related to water permeation at a given reference temperature. Consequently, the deployment of such analytical models provides indispensable predictive capabilities regarding material degradation kinetics under hygrothermal aging. The Arrhenius formulation is equally vital for estimating the apparent activation energy for moisture diffusion and quantifying the degradation rate.

Overall, these multifaceted approaches offer profound insights into the physical and chemical degradation micromechanisms of adhesively bonded joints, ultimately facilitating the development and optimization of highly durable composite structures. The service life of structural adhesive joints is governed by several critical environmental factors, notably moisture concentration, thermal gradients, fire exposure, and ultraviolet (UV) radiation [7].

Table 3 details the exposure environments and the corresponding water diffusion parameters for various structural adhesive joints as reported in the literature. The fundamental diffusion kinetics are broadly classified into Fickian, Dual-Fickian, and Langmuir models. This comprehensive summary also highlights that water diffusion parameters exhibit substantial variability depending heavily on the specific chemical formulation of the adhesive and the exact environmental aging conditions.

Table 3 Water Diffusion Parameters Reported in Previous Literature

Adherend/Adhesive	RH (%)	Temp. (°C)	Initial D (10^-7 mm²/s)	$Mmax$ (%)	Diffusion behavior
Al/Epoxy FM 73 [65]	95.8	50	5.0	2.2	Fickian
	79.5	70	79.0	2.5	
Al/epoxy EA9321 [66]	95.8	50	3	3.8	Fickian
Steel/AV119 epoxy [67]	95.8	50	2.4	5.0	Fickian/
	81.2	50	2.4	3.1	Dual Fickian
Al/Epoxy FM 73 [68]	100	50	7.18	3.75	Fickian
Al/epoxy FM 1000 [69]	65	25	2.4	3.0	Fickian
	95	25	2.4	6.0	
	95	50	3.4	13.4	

[Downloaded from rds.iust.ac.ir on 2026-11-19]

[DOI: 10.22068/ase.2026.741]

Al/AV138/2015 [15]	30	25	0.15	2.29	Fickian
	75.3	25	0.22	2.97	
Steel/ Hysol 3425 [70]	100	50	0.74	4.5	Fickian
Al/ epoxy 4532 [71]	30	65	5.1	0.42	Fickian
	60	65	8.0	2.1	
Al/ toughened epoxy [72]	95	40	13.4	4.78	Fickian/
	82	40	14.2	3.55	Dual Fickian/
	75	40	15.9	2.79	Langmuir
	43	40	11.3	1.65	
	31	40	13.9	1.26	
CFRP/GFRP/ steel/ epoxy adhesive [73]	100	45	4.28	1.34	Fickian/
	100	20	0.35	1.36	Dual Fickian
	95	45	6.02	1.10	
CFRP/epoxy SY14 [74]	100	90	62.8	8.13	Fickian
Al/epoxy EA9346 [75]	100	67	2.2	5.3	Fickian
CFRP/epoxy FM300 [76]	100	70	6.76	1.24	Fickian

3.3. Summary of section

In this section, the procedures and governing theories underlying the various stages of the problem investigated in this review article have been comprehensively discussed. Furthermore, specific theoretical frameworks accounting for the dissimilarity of the adherends, including the methodologies for calculating and applying moisture conditions, were introduced. Additionally, the fundamental mechanisms of the Cohesive Zone Model (CZM) were briefly outlined.

4. A review of the research background

Adhesively bonded joints with composite adherends have gained significant prominence across diverse industries due to a combination of factors, including exceptional strength-to-weight ratios, outstanding durability, and superior corrosion resistance. However, their long-term degradation can compromise structural integrity and safety, necessitating robust degradation prediction methodologies.

The following discourse provides a critical review of existing research concerning:

- The application of Cohesive Zone Modeling (CZM) for predicting adhesive behavior.
- The impact of hygrothermal conditions on adhesive performance.

[Downloaded from rds.iust.ac.ir on 2026-11-19]

[DOI: 10.22068/ase.2026.741]

- The efficacy of nanoparticle reinforcement in enhancing environmental resistance.
- Digital Image Correlation (DIC) approaches for constitutive law determination.

The primary objective is to identify existing gaps in the literature and highlight potential research areas to address these deficiencies.

4.1. Cohesive Zone Model (CZM) in Adhesive Joints

The Cohesive Zone Model (CZM) aims to characterize failure mechanisms through the implementation of traction-separation laws (TSLs). Generally, cohesive zone models are categorized into two primary frameworks: potential-based models, which are energy-driven, and effective traction-displacement models.

In potential-based models, the traction-separation laws are derived using fracture energy potential functions. Conversely, in non-potential-based models, these relationships are developed based on effective displacement and traction vectors. Consequently, various models have been proposed to simulate material behavior under different loading modes, as illustrated in Figure 15 [77].

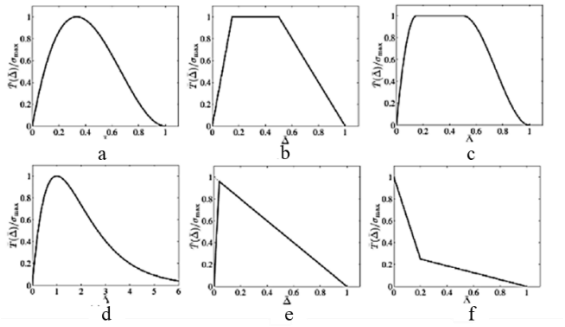


Figure 15 Models of the law of attraction-separation: a) Polynomial b) Trapezoidal c) Smooth trapezoidal d) Exponential e) Bilinear f) Smooth bilinear [77].

In 2010, Carlberger and Stig [78] evaluated the response of steel and aluminum top-hat and H-shaped components joined using two different epoxy adhesives. In the context of reducing vehicle mass, the bonded specimens were examined under dynamic conditions through drop-weight impact experiments performed at an impact speed of 9 m/s. For the numerical representation of the adhesive joint, a bilinear cohesive zone model (CZM) was adopted.

According to the results presented in Figure 16, the numerical simulations differed from the experimental observations by approximately 10%. This close agreement was mainly associated with the use of a suitable constitutive description capable of accurately characterizing the adhesive interface behavior.

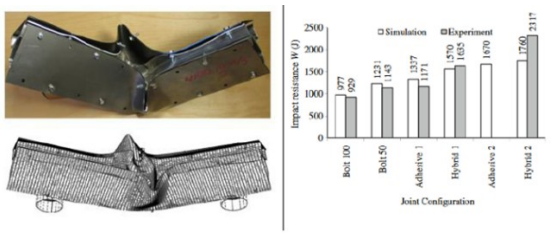


Figure 16 Left: Experimental and numerical hat-shaped specimen, right: Damage resistance at different joints [78].

Later, in 2015, May et al. [79] carried out an extensive investigation into the performance of a crash-tolerant adhesive under a wide spectrum of strain rates, ranging from 0.067 s^{-1} to 104 s^{-1}. They introduced a strain-rate-sensitive cohesive zone model in which both the damage initiation stress and the fracture energy vary as functions of strain rate. As shown in Figure 17, the proposed formulation was based on a bilinear traction–separation relation for Mode I and a trapezoidal constitutive relation for Mode II.

[Downloaded from rds.iust.ac.ir on 2026-11-19]

[DOI: 10.22068/ase.2026.741]

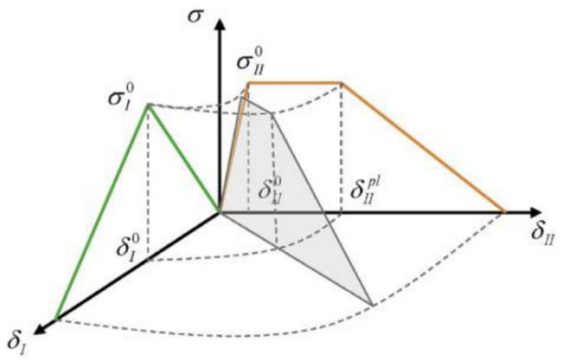


Figure 17 Combined bilinear and trapezoidal tension-separation law [79].

Subsequently, in 2019, Gheibi et al. [80] utilized a bilinear CZM to extract the material constants for an automotive structural adhesive. To evaluate the adhesive fracture energy, several data interpretation techniques were examined, among which Modified Beam Theory (MBT) and Compliance-Based Beam Theory (CBBT) received particular attention. The comparison indicated that CBBT provides greater reliability and is better suited for measurements performed at the laboratory scale. In addition, the numerical predictions generated using the cohesive zone model showed strong agreement with the corresponding experimental observations.

In a study conducted in 2021, Peres et al. [81] explored how the overlap length and the adhesive formulation influence the behavior of composite Single Lap Joints (SLJs) subjected to dynamic impact conditions. Their work combined experimental testing with numerical simulations based on the cohesive zone model. The outcomes revealed that, in the case of more compliant and ductile adhesives, extending the overlap length markedly improves the load-carrying capacity of the joint.

4.2. Environment-Dependent Cohesive Zone Models

The Cohesive Zone Model (CZM) serves not only as a robust tool for simulating the baseline performance of adhesive joints but has also been increasingly adopted in recent years to characterize the influence of environmental conditions on joint integrity.

In 2007, Liljedahl et al. [65] employed the CZM to investigate aluminum Single Lap Joint (SLJ) and End Notched Flexure (ENF) specimens bonded with an epoxy-based adhesive under humid conditions. Their methodology involved an initial extraction of cohesive zone parameters from experimental data, which were subsequently utilized to predict the residual strength of joints with diverse geometries.

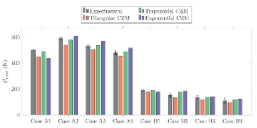
In a concurrent study [82], the authors utilized the CZM to evaluate composite-to-composite, aluminum-to-aluminum, and hybrid composite-to-aluminum joints subjected to the synergistic effects of moisture and mechanical stress. Their findings indicated that the simultaneous exposure to these conditions accelerates the degradation of mechanical properties. It was also reported that non-identical (hybrid) single-lap joints (SLJs) developed greater residual stresses than similar-material joints. This behavior was mainly associated with the discrepancy in the coefficients of thermal expansion (CTE) of the two adherends.

In 2018, Costa et al. [83] investigated how moisture ingress contributes to the mechanical deterioration of adhesive joints by employing Double Cantilever Beam (DCB) specimens. Their study was aimed at quantifying the loss of tensile strength and fracture energy in two different adhesive systems. Based on the experimental observations, empirical constitutive expressions were formulated to predict the reduction in mechanical performance as a function of the level of absorbed moisture. As shown in Figure 18, these formulations, which were established on the basis of moisture concentration and Fickian diffusion behavior, revealed that increasing moisture uptake leads to a reduction in both joint strength and fracture

[Downloaded from rds.iust.ac.ir on 2026-11-19]

[DOI: 10.22068/ase.2026.741]

energy, while the failure strain, and thus the ductility, increases. When this degradation framework was incorporated into the cohesive zone model (CZM), the predicted failure loads of adhesive joints exposed to humid conditions matched the experimental results with high accuracy.



Definition of each aged stage for both studied adhesives.

	Nagase XNR 6852-1	SikaPower 4720
RH = 0%	Case A1	Case B1
RH = 25%	Case A2	Case B2
RH = 40%	Case A3	Case B3
RH = 60%	Case A4	Case B4

Figure 18 Comparison of experimental and numerical results of the failure force for different samples (right table) and different viscous zone models [83].

In 2019, Machado et al. [84] studied the effects of temperature and strain rate on the Mode I fracture energy of CFRP DCB specimens. The experimental program involved falling-wedge impact tests performed at an impact speed of 4.7 m/s. According to the results presented in Figure 19, temperature had a substantial effect on the fracture energy, whereas the influence of strain rate was comparatively limited.

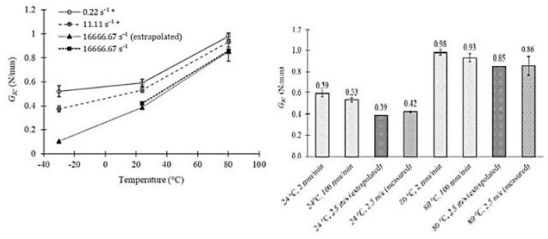


Figure 19 Right: Failure energy in dynamic and static tests at 24 and 80 degrees Celsius, left: Failure energy as a function of temperature at different strain rates [84].

Later, in 2020, Li et al. [85] investigated the damage mechanisms, impact energy dissipation, and residual load-bearing performance of adhesively bonded single-lap joints (SLJs) subjected to different temperature conditions and impact energy levels. Their numerical analysis was based on a bilinear cohesive zone model (CZM). The force–displacement responses were obtained from Double Cantilever Beam (DCB) and End-Notched Flexure (ENF) experiments with the aid of Digital Image Correlation (DIC). In addition, the cohesive properties and the resistance curve (R-curve) were identified. The study showed that when the service temperature moves closer to the adhesive glass transition temperature (T_g), the joint experiences a marked reduction in both absorbed energy and residual load-carrying capability.

Also in 2020, Joher et al. [86] examined aluminum DCB, ENF, and Mixed-Mode Flexural (MMF) adhesive joints bonded with Araldite 2015 under humid conditions in order to evaluate how varying strain rates influence fracture energy. Based on the assumption that higher loading rates can promote interfacial degradation, they applied the CZM framework to establish a numerical model capable of predicting joint response. Their results indicated strong agreement between the experimental observations and the numerical predictions.

In 2023, Du et al. [54] proposed a CZM specifically for strain-rate-sensitive materials to simulate the failure of steel top-hat specimens under various impact velocities and temperatures. In this framework, the separation energy and peak stress are formulated as functions of strain rate and temperature. The model constants were derived from a hybrid approach combining experimental data and simulations. As shown in Figure 20, the results emphasized that both separation energy and peak stress are highly dependent on temperature and strain rate, highlighting the necessity of incorporating these variables to ensure modeling accuracy.

[Downloaded from rds.iust.ac.ir on 2026-11-19]

[DOI: 10.22068/ase.2026.741]

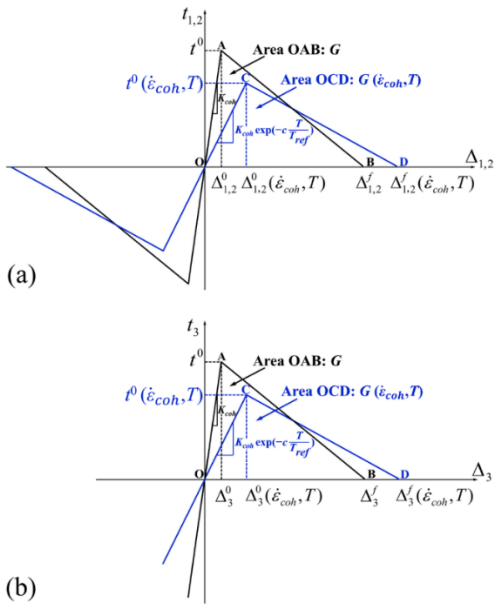


Figure 20 Tension-separation law considering the effects of strain rate and temperature, top: Modes II and III, bottom: pure Mode I [54].

A summary of selected research on adhesive joint modeling using the Cohesive Zone Model is presented in Table 4.

Table 4 Selected research in the field of Cohesive Zone Modeling (CZM) for adhesive joints.

Year	Ref.	Authors	Traction-Separation Law (TSL)	Environmental Condition	Key Findings
2009	[87]	Marzi et al.	Trapezoidal	-	Proposed a new model accounting for strain rate and adherend plasticity.
2010	[78]	Carlberger et al.	Bilinear	-	Investigated dissimilar top-hat specimens under dynamic loading.
2015	[79]	May et al.	Bilinear – Trapezoidal	-	Examined strain rate effects on initiation stress and fracture energy.
2019	[80]	Gheibi et al.	Bilinear	-	Extracted constants for an automotive adhesive; compared data reduction methods.
2019	[88]	Valente et al.	Bilinear	-	Used CZM to determine the optimal adhesive-adherend combination.
2019	[89]	Lissner et al.	Trapezoidal	-	Developed a model considering strain rate and adhesive layer thickness.
2020	[90]	Machado et al.	Trapezoidal	-	Extracted constants for composite DCB specimens at varying strain rates.
2018	[83]	Costa et al.	Bilinear	Moisture	Investigated the effect of moisture diffusion on DCB mechanical properties.
2019	[15]	Zaeri & Saeidi	Bilinear	Moisture	Studied 1K and 2K adhesive DCB joints under humid conditions.
2019	[84]	Machado et al.	Bilinear	Temperature	Analyzed the effect of temperature and strain rate on composite DCB fracture energy.
2020	[85]	Li et al.	Bilinear	Temperature	Determined energy absorption and failure force of SLJs post-impact at various temperatures.

[Downloaded from rds.iust.ac.ir on 2026-11-19]

[DOI: 10.22068/ase.2026.741]

2020	[86]	Joher et al.	Bilinear	Moisture	Investigated the synergistic effects of strain rate and moisture on adhesive joints.
2023	[54]	Du et al.	Bilinear	Temperature	Proposed a CZM for strain-rate-sensitive materials under dynamic and thermal loading.

4.3. Temperature Effects on Adhesive Joints

Automotive body structures are exposed to a broad spectrum of service temperatures, typically from $-40°C$ to $80°C$, although the exact range varies with component position, distance from the engine bay, and surrounding environmental conditions. Under particularly severe operating conditions, the temperature may rise beyond these limits. Variations of this kind can markedly influence the physicochemical characteristics of structural adhesives and, as a result, alter their mechanical response [91].

Among the thermal parameters affecting adhesive performance, the glass transition temperature (T_g) plays a central role. When the service temperature approaches this critical threshold, the adhesive gradually changes from a stiff, glass-like material into a softer and more deformable rubber-like phase. This transformation is generally accompanied by a decline in stiffness, strength, and resistance to interfacial failure, thereby reducing both the load-carrying capability of the joint and the effectiveness of adhesion [92]. Because of this, the influence of temperature on bonded joints has been widely examined in the literature, and several important observations are outlined below.

Bauwens and co-workers [93, 94] presented two influential studies in 1972 addressing the dependence of polymer behavior on temperature and strain rate. Their work examined the link between yield stress and loss tangent, as well as the relationship between stored energy and dissipated energy under different thermo-mechanical conditions. By characterizing the variation of loss tangent with temperature and strain rate, they were able to predict compressive stress-strain responses under constant loading conditions, and the predicted curves showed strong agreement with experimental data.

Later, Banea et al. [95] analyzed the Mode I fracture energy of an epoxy adhesive used in automotive applications over an extended temperature interval. Their findings confirmed that fracture energy is highly sensitive to temperature changes. In particular, as illustrated in Figure 21, a pronounced dro87p in fracture energy was observed once the temperature exceeded the glass transition temperature (T_g).

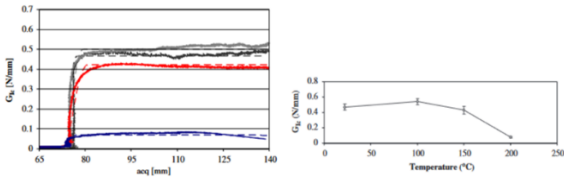


Figure 21 Right: Effect of temperature on the fracture energy of 1244-XN adhesive Left: R-Curve for experimental and numerical DCB samples as a function of temperature [95].

Blackman et al. [96] reported in 2000 on the fracture energy behavior of several adhesives tested at temperatures of 23°C and -40°C under a separation velocity of 2 m/s using Tapered Double Cantilever Beam (TDCB) specimens. Their results demonstrated a consistent decline in Mode I fracture energy for all investigated adhesives as the temperature decreased. In 2008, Adamvalli et al. [97] investigated the mechanical performance of titanium Single-Lap Joints (SLJs) bonded with Araldite 2014 over a temperature interval from 25°C to 100°C by means of a Split-Hopkinson Pressure Bar (SHPB). The study

[Downloaded from rds.iust.ac.ir on 2026-11-19]

[DOI: 10.22068/ase.2026.741]

revealed that increasing temperature adversely affects joint strength, with the bonded joints exhibiting approximately 35% lower strength at 100°C than at ambient conditions.

Carlberger et al. [98], in 2009, analyzed the influence of both temperature and strain rate on Mode I and Mode II fracture energies of the automotive adhesive Betamate 1044xv. Their findings highlighted that, due to the adhesive's viscoelastic response, these two parameters are strongly interrelated. This correlation, commonly described through the time–temperature superposition principle, suggests that thermal experiments may serve as practical alternatives to dynamic impact testing. In 2017, Machado et al. [99] experimentally explored the effects of temperature and strain rate on Mode I fracture behavior in CFRP DCB specimens. Their observations confirmed that both factors significantly affect the fracture energy of the bonded interface. As shown in Figure 22, lower temperatures combined with higher strain rates generally lead to diminished fracture energy.

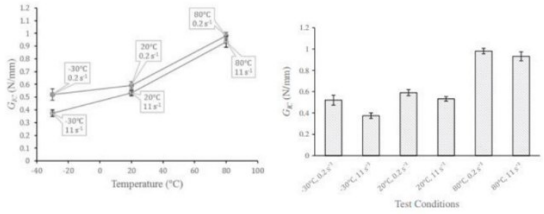


Figure 22 Fracture energy as a function of temperature and strain rate [99].

4.4. Moisture Effects on Adhesive Joints

Moisture penetration is widely recognized as one of the most influential factors responsible for the long-term deterioration of adhesive joint mechanical performance [100]. Under humid service conditions, water molecules diffuse into the adhesive polymer network and, much like the effect of increased temperature, modify the response of the bonded assembly and reduce its load-carrying capability, especially when subjected to impact forces [101]. Numerous studies have therefore focused on evaluating the role of moisture in altering adhesive behavior under static and quasi-static loads, as well as on the combined influence of temperature and humidity, commonly referred to as hygrothermal aging. Key contributions in this area are summarized below.

Kinloch et al. [102] examined aluminum TDCB specimens bonded with an epoxy adhesive in 2000. By comparing fracture energy values obtained in dry and moisture-conditioned states, they showed that surface treatment plays a decisive role in joint durability. In particular, the use of a primer before bonding improved resistance to humid environments by filling microscopic surface voids and promoting stronger interfacial bonding.

Later, Liljedahl et al. [103] investigated moisture uptake in bulk adhesive samples in 2012. Their study showed that water absorption substantially impairs the mechanical characteristics of the adhesive. This degradation was mainly attributed to plasticization, which causes a reduction in the glass transition temperature (T_g). As a consequence, the adhesive exhibits lower stiffness, reduced yield strength, and a decrease in Poisson's ratio, while its strain to failure increases, indicating enhanced ductility.

Similarly, Moazzami et al. [104] analyzed the moisture diffusion response of bulk epoxy adhesives exposed to cyclic environmental conditions in 2020. Their results demonstrated that higher equilibrium moisture content (M_∞) and larger diffusion coefficients (D) are associated with significant losses in tensile strength and elastic modulus.

It should also be emphasized that moisture-related degradation is not confined to the adhesive layer or the adhesive/adherend interface. The adherends themselves, especially

[Downloaded from rds.iust.ac.ir on 2026-11-19]

[DOI: 10.22068/ase.2026.741]

when made of composite materials, are also susceptible to moisture absorption. In such cases, water ingress may deteriorate the matrix resin, weaken fiber–matrix bonding, and cause hygroscopic expansion in the laminate structure [105].

As noted earlier, the response of an adhesive in bulk form may differ considerably from its behavior when constrained within an actual bonded joint. In this context, Viana et al. [106] used DCB specimens in 2017 to determine both the absorbed moisture content and the corresponding fracture energy of the joint. They also developed a numerical approach for estimating the diffusion coefficient at the adhesive/adherend interface as a function of aging duration. The influence of moisture uptake on the fracture energy of two different adhesive systems is presented in Figure 23.

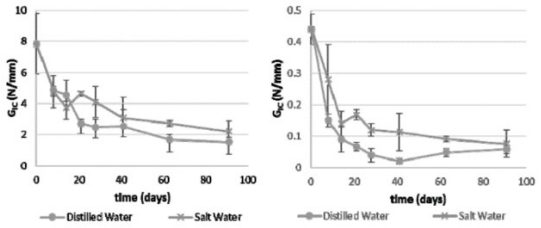


Figure 23 Effect of moisture absorption on the fracture energy of two adhesive samples, right: Sikapower4720, left: XNR6852 [106].

In 2013, Perez-Pacheco et al. [107] evaluated the effect of humid environments on the mechanical properties and failure modes of unidirectional (UD) composites. Specimens were exposed to relative humidity (RH) levels of 25%, 55%, and 95%, with some surfaces treated with a primer. Their findings confirmed that moisture absorption leads to a decline in T_g and mechanical performance. However, the application of a primer was found to reduce the sensitivity of the composite's mechanical properties to environmental stressors under tensile loading.

4.5. Adhesively Bonded Joints Aged Under Hygrothermal Conditions

The study of adhesively bonded joints under hygrothermal conditions involves investigating how material properties and the bonding process influence the residual strength of aged joints. Various factors, including surface preparation, water ingress (moisture diffusion), and experimental methodologies, can significantly affect joint performance and lead to failure in hygrothermal environments. These parameters influence the overall characteristics and structural integrity of the aged assembly. Consequently, understanding the complex interplay between these factors is crucial for optimizing adhesive joints across diverse applications. The following review of prior research provides a comprehensive discourse on these variables and emphasizes the necessity for further investigation to enhance the fidelity of predictive models for joint performance.

In 2014, Jiang et al. [108] carried out an experimental study on the mechanical performance of adhesive joints in Fiber Reinforced Polymer (FRP) sandwich structures after hygrothermal aging. Their observations showed that, when subjected to shear loading, failure predominantly took place as cohesive rupture inside the adhesive layer. In contrast, under tensile and mixed-mode loading, damage was mainly associated with fiber crushing and delamination within the composite adherends.

In 2019, Mariam et al. [109] evaluated how hygrothermal aging influences adhesive joints made from both similar and dissimilar adherends, namely AA7075 aluminum alloy and Glass Fiber Reinforced Epoxy (GFRE). The study demonstrated that longer exposure to hygrothermal conditions led to greater moisture uptake in the bonded region. At the same time, the mechanical strength of the joints gradually declined, which in turn promoted different failure

[Downloaded from rds.iust.ac.ir on 2026-11-19]

[DOI: 10.22068/ase.2026.741]

patterns. As presented in Figure 24, the fracture surfaces exhibited a range of damage mechanisms, including cohesive failure, adhesive failure, structural failure, and interlaminar failure.

In 2022, Moazzami et al. [110] explored the influence of cyclic hygrothermal aging on the Mode I fracture energy of dissimilar adhesive joints using the Double Cantilever Beam (DCB) configuration. Their results indicated a reduction in fracture energy with increasing moisture absorption and longer environmental exposure. Nevertheless, during the desorption or drying stage, part of the lost fracture energy was restored as drying progressed. According to Figure 25, the Mode I fracture energy throughout both absorption and desorption stages depended on the combined effects of moisture concentration and the number of aging cycles. It was also reported that specimens containing higher levels of moisture were less affected by aging cycles than dry samples. Moreover, increasing the number of cycles reduced the extent to which additional cycling influenced the Mode I fracture energy.

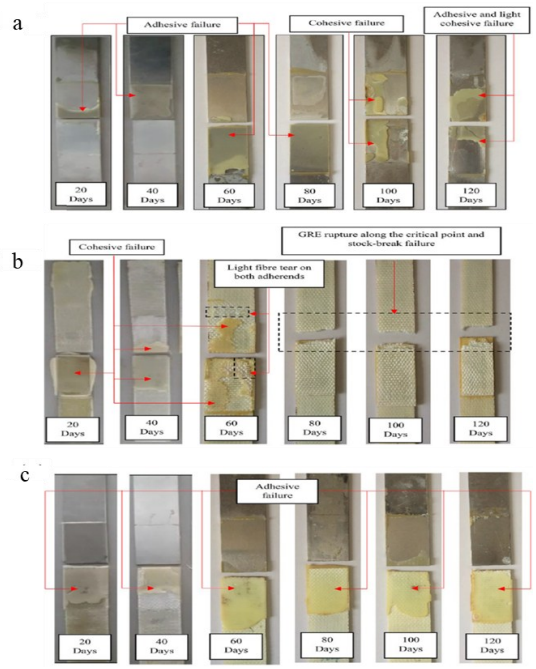


Figure 24 Failure mode of aged specimen: (a) homogeneous - AA7075/AA7075, (b) homogeneous - GRE/GRE, and (c) heterogeneous - AA7075/GRE [109].

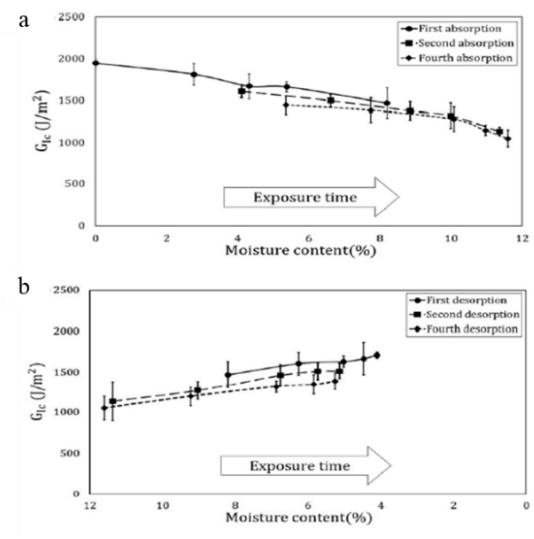


Figure 25 Change in failure energy of Mode I loading in the absorption of different moistures in the processes of (a) absorption (b) desorption [110].

In In 2024, Yu et al. [111] developed an analytical framework to investigate degradation-related failure behavior in adhesively bonded corrugated sandwich structures (ABCSS) exposed to three-point bending and hygrothermal aging conditions. The stress profiles in the adhesive layer at different immersion durations in deionized water at 50°C are presented in Figure 26.

As shown in Figure 26, hygrothermal exposure alters the initially uniform stress pattern in the adhesive layer as a result of progressive material degradation. The highest stress level throughout the adhesive layer was observed after 100 days of aging. In addition, stress values in the flat region of the adhesive were generally greater for aged specimens than for the unaged configuration, whereas the fillet region exhibited lower stress levels after hygrothermal aging compared with the non-aged condition.

[Downloaded from rds.iust.ac.ir on 2026-11-19]

[DOI: 10.22068/ase.2026.741]

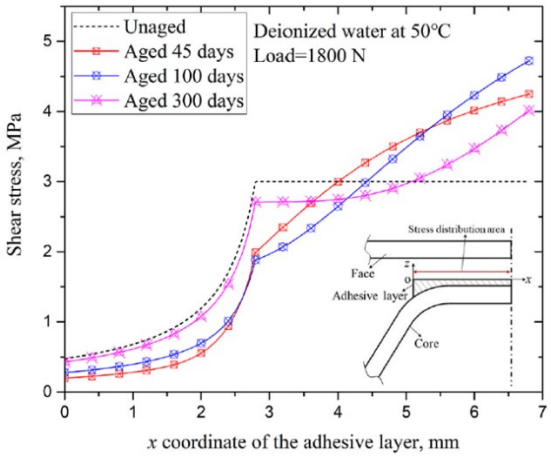


Figure 26 Shear stress distribution of the adhesive layer for different aging periods [111].

Table 5 summarizes the Traction-Separation Law (TSL) parameters specifically fracture toughness (G_c), cohesive strength (T_{max}), and failure displacement (δ_F) extracted from various experimental studies on adhesive joints subjected to hygrothermal aging.

As indicated in the table, for metallic joints such as Al/2015 and Al/AV138, the Mode I fracture energy (G_I) and cohesive strength exhibit a significant decline as the Relative Humidity (RH) increases. Conversely, for composite systems like CFRP/epoxy and CFRP/epoxy SY14, the Mode I fracture toughness remains relatively stable across varying RH levels. However, a universal trend observed across all four joint configurations is that elevated temperatures consistently lead to a reduction in Mode I fracture toughness.

Regarding Mode II fracture behavior, the fracture toughness of Al/2015 and Al/AV138 decreases synergistically with both increasing temperature and RH. For CFRP/epoxy and CFRP/epoxy SY14, while Mode II toughness is comparatively insensitive to RH fluctuations, it undergoes a marked degradation at higher temperatures.

Overall, the TSL parameters derived from prior literature underscore the profound impact of hygrothermal aging on the fracture envelope of adhesive joints. These empirically determined parameters are essential input variables for Cohesive Zone Modeling (CZM), enabling the reliable prediction of structural failure in joints operating under adverse environmental conditions.

Table 5 Hygrothermal Traction-Separation Law (TSL) parameters derived from various literature sources.

Adherend/Adhesive	RH (%)	Temp. (°C)	Mode I: G_I (N/mm)	Mode I: T_I (MPa)	Mode I: δ_{II} (mm)	Mode II: G_{II} (N/mm)	Mode II: T_{II} (MPa)	Mode II: δ_{III} (mm)	Ref.
Al/2015	30	25	0.57	21	-	4.87	18	-	[15]
	75.3	25	0.35	12	-	2.98	12	-	
	84.2	25	0.37	10	-	2.16	10	-	
	100	25	0.23	6	-	0.70	6	-	
Al/AV138	30	25	0.26	39	-	0.44	30	-	[15]
	75.3	25	0.12	30	-	0.21	32	-	
	84.2	25	0.16	24	-	2.24	36	-	
	100	25	0.19	18	-	2.10	25	-	
CFRP/epoxy	95	45	0.94	22.3	0.136	5.98	20.2	0.577	[73]

[Downloaded from rds.iust.ac.ir on 2026-11-19]

[DOI: 10.22068/ase.2026.741]

	100	45	0.63	17.2	0.128	5.54	18.6	0.578	
	100	45	0.70	19.1	0.118	6.27	21.8	0.639	
CFRP/epoxy SY14	20	22	1.2	66	-	2.5	40	-	[74]
	100	22	0.53	33	-	1.2	20	-	
	20	95	0.7	38	-	1.4	23	-	
	100	95	0.3	15	-	0.6	10	-	
CFRP/epoxy	85	70	0.65	55	0.008	0.75	39	0.030	[112]
	85	70	0.62	45	0.600	3.00	37	0.250	
	85	70	0.25	44	0.200	3.15	35	0.150	

4.6. Effect of Nanoparticles on Enhancing Adhesive Resilience Against Environmental Conditions

The use of nanoparticles as modifiers in structural adhesives has gained considerable attention as an effective approach for improving adhesive performance, especially when exposed to harsh service environments. In engineering applications, structural adhesives are widely valued because they enable more homogeneous stress transfer and allow reliable joining of materials with different properties. Nevertheless, as noted earlier, their durability over extended periods can be adversely affected by environmental factors, including humidity and thermal variations. Overall, the incorporation of nanoscale reinforcements represents an efficient means of enhancing both the mechanical behavior and the environmental durability of adhesive systems, thereby supporting the design of sustainable and high-performance bonding materials.

In 2014, Gkikas et al. [113] examined the effects of Multi-Walled Carbon Nanotube (MWCNT) incorporation into adhesives with respect to lap shear performance, galvanic corrosion behavior, and resistance to environmental degradation. Their objective was to assess whether the degradation behavior of MWCNT-modified adhesives under environmental exposure is influenced by either nanoparticle concentration or substrate material. The results showed that incorporating 0.1 wt% MWCNT into the epoxy system reduced the galvanic interaction between Al 2024 and the neat epoxy. In contrast, when the MWCNT content was increased to 0.5 wt%, the galvanic effect in the aluminum/neat epoxy configuration became markedly more severe.

In 2018, Khoramishad et al. [114] investigated how temperature affects the fracture strength of adhesive joints enhanced with MWCNTs by employing Double Cantilever Beam (DCB) specimens. As presented in Figure 27, their results demonstrated that the reinforcing contribution of MWCNTs decreases to some extent as the testing temperature rises. Moreover, beyond a certain critical temperature, the inclusion of these nanoparticles can adversely affect the shear strength of both DCB and Single Lap Joint (SLJ) specimens. By applying a mathematical modeling approach, the authors also determined the optimum MWCNT weight fractions for adhesive systems subjected to different temperature conditions.

[Downloaded from rds.iust.ac.ir on 2026-11-19]

[DOI: 10.22068/ase.2026.741]

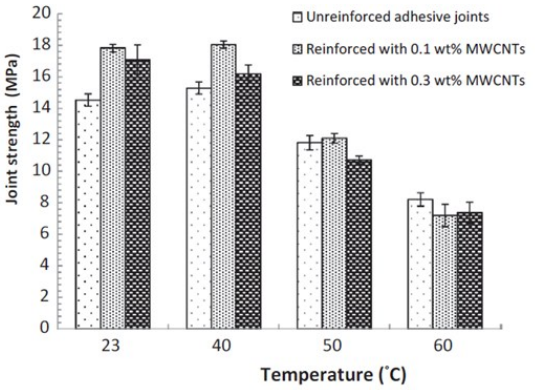


Figure 27 Effects of MWCNT weight percentage and test temperature on the strength of adhesive joints [114].

In 2023, Hajizamani et al. [115] introduced an epoxy adhesive reinforced with $Ti_3C_2T_x$ MXene nanoparticles, evaluating the tensile and shear strength of the adhesive film in aluminum joints. They also assessed the thermal stability of the adhesive in the presence of MXene. The results demonstrated that incorporating 1.0 wt% of inorganic MXene nanoparticles into an epoxy/phenolic resin blend led to improvements of 16.49% in tensile strength, 43.51% in modulus, and 17.19% in toughness. Furthermore, as shown in Figure 28, the addition of 1.0 wt% MXene induced a shift toward a cohesive failure mode.

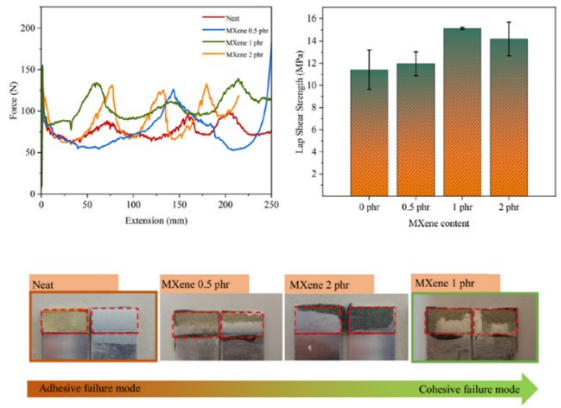


Figure 28 Failure mode of epoxy adhesive joints and epoxy film containing MXene [115].

Esmail et al. [116] examined how the incorporation of Single-Walled Carbon Nanotubes (SWCNTs) and Fullerene nanoparticles affects the shear performance of CFRP single-lap joints (SLJs) under both initial and hygrothermally aged conditions. Their findings showed that the presence of nanoparticles, with Fullerene being especially effective, decreased moisture uptake and consequently improved the lap shear strength of the bonded joints. Although exposure to hygrothermal environments led to a decline in the shear strength of neat epoxy and systems containing only one type of nanofiller, the adhesive joints modified with a hybrid combination of Fullerene and SWCNTs demonstrated an increase in strength. In terms of fracture behavior, the joints generally exhibited a mixed adhesive–cohesive failure pattern. Nevertheless, both hygrothermal aging and nanoparticle incorporation contributed to a larger proportion of cohesive failure, indicating improved integrity within the adhesive layer.

In another work, Farzanehfar et al. [117] introduced an advanced epoxy-based nanocomposite adhesive containing Silica Nanoscale Ionic Materials (SiO_2-NIMs), prepared via a solvent-free route, which resulted in improved bonding performance and greater thermal resistance. As shown in Figure 29, the fracture characteristics varied significantly among the tested systems: neat epoxy predominantly failed adhesively, the SiO_2/EP adhesive displayed a mixed adhesive/cohesive mode, whereas the SiO_2-NIMs/EP nanocomposite showed fully cohesive failure. For the SiO_2-NIMs/EP adhesive, residual adhesive material remained attached to the aluminum surface after failure, confirming that fracture occurred within the adhesive bulk rather than at the interface. This behavior reflects stronger interfacial interaction and better

[Downloaded from rds.iust.ac.ir on 2026-11-19]

[DOI: 10.22068/ase.2026.741]

compatibility with the substrate relative to the other formulations.

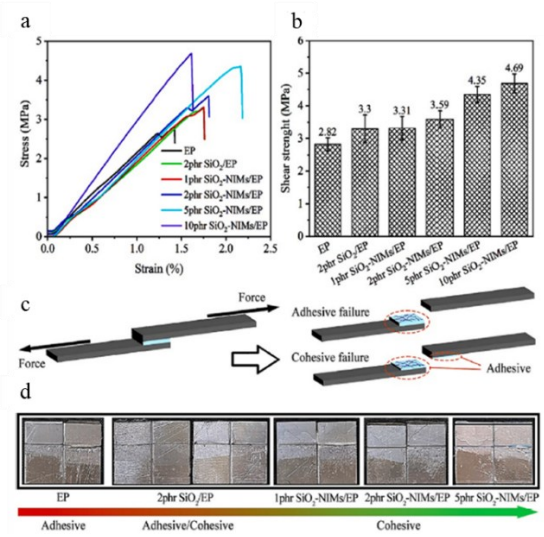


Figure 29 a) Stress-strain curves b) shear strength results of pure epoxy, SiO_2/EP (2 wt%) and SiO_2-NIMs/EP (1, 2, 5 and 10 wt%) c) adhesive and cohesive failure modes. d) Failure images and failure modes of pure epoxy, SiO_2/EP (2 wt%) and SiO_2-NIMs/EP (1, 2, 5 and 10 wt%) [117].

In 2023, Ceylan et al. [118] evaluated the adhesion between AA7075-T6 aluminum (treated via FPL etching) and epoxy adhesives reinforced with Boron Nitride Nanopowder (BNNP), Alumina Nanopowder (ANP), and MWCNTs in SLJ configurations. The bonded assemblies were exposed to hygrothermal conditioning at 60°C and 100% relative humidity for periods extending to six weeks. Among all nanofiller-modified systems, the MWCNT-containing joints consistently preserved the greatest proportion of their shear strength throughout the aging process, while ANP- and BNNP-modified adhesives ranked second and third, respectively. After two weeks of exposure, the average shear strength of the neat adhesive joint decreased by 64.72%. In contrast, the corresponding reductions for joints reinforced with BNNP, ANP, and MWCNTs were 61.11%, 56.31%, and 39.34%, respectively.

More recently, Ejaz et al. [119] reported an experimental assessment in 2024 on the influence of MWCNTs and graphene nanoplatelets (GNPs) incorporated at 0.25, 0.5, 0.75, and 1 wt% on the mechanical behavior of both SLJ and double strap joint (DSJ) configurations. Their findings indicated that SLJ and DSJ specimens reinforced with MWCNTs were mainly characterized by adhesive failure regardless of nanoparticle content. In contrast, DSJ specimens displayed a noticeable difference in failure behavior when GNPs were used instead of MWCNTs. As illustrated in Figure 30, DSJ samples containing MWCNTs predominantly failed adhesively, whereas GNP-modified SLJ and DSJ specimens tended to exhibit cohesive failure at lower filler loadings, followed by a transition toward adhesive failure when the concentration reached 1 wt%.

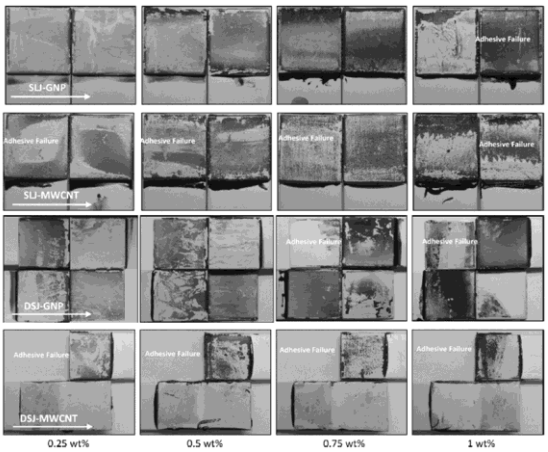


Figure 30 Failure modes of SLJ and DSJ specimens [119].

Numerous studies have investigated the influence of various nanoparticles on the Lap Shear Strength (LSS) of epoxy adhesives. A comprehensive summary of recent research focused on the enhancement of the shear performance of epoxy-based systems through the incorporation of diverse nanofillers is consolidated in Table 6.

[Downloaded from rds.iust.ac.ir on 2026-11-19]

[DOI: 10.22068/ase.2026.741]

Table 6 Effect of various nanoparticles on the lap shear strength of epoxy adhesives

Nanoparticle	Content (wt.%)	Adherents	Lap shear strength change (%)	Ref
MWCNT and nanoclay	0.5, 1 and 1.5	aluminum	52	[120]
alumina	5 and 10	aluminum	15	[121]
alumina	0.5, 1.0, 1.5 and 2.0	aluminum	52 at 1.5 wt.%	[122]
silica	10	stainless steel	20	[49]
SWCNTs	1	carbon fiber reinforced plastics	-10	[123]
elastomeric nanoparticles	20	aluminum	98	[124]
		copper	93	
		steel	18	
MWCNT	1	aluminum	53	[125]
SWCNTs	0.5		46	
graphene	0.5		49	
MWCNT	0.5	steel	39	[126]
MWCNT	1	glass fiber/epoxy composites	7	[127]
graphene	0.5	steel	-21	[128]
graphene	1	aluminum	-14	[129]
montmorillonite clay	2	steel	40	[130]
	5		65	
HNT@SiO2 core/shell	2	Steel-epoxy/carbon fiber	130	[38]
Fe3O4	1	epoxy plastic slides	19	[47]
silver plating nano-graphite	20	carbon steel	8	[131]
TiO2	10	mild steel-aluminum	62	[132]
Zirconia	1 vol.%	aluminum	60	[133]
nano-Al2O3	1.5	aluminum	70	[134]
MWCNT	3	aluminum	50	[134]
Poss	3	aluminum	46	[135]
Clay	1	Glass/epoxy composite	7	[36]

[Downloaded from rds.iust.ac.ir on 2026-11-19]

[DOI: 10.22068/ase.2026.741]

graphene	1	aluminum	-125	[129]
Peptide Nanotube	5	aluminum	67	[136]

5. Conclusion

This review has synthesized the critical challenges and advancements in the field of adhesively bonded composite joints subjected to hygrothermal exposure. The primary conclusions are as follows:

- Environmental Sensitivity: Hygrothermal aging remains a formidable barrier to the widespread use of composite adhesive joints, as moisture ingress induces plasticization, lowers the glass transition temperature (T_g), and significantly reduces the load-bearing capacity.
- Nanotechnology as a Solution: The integration of specialized nanoparticles, such as Multi-Walled Carbon Nanotubes (MWCNTs) and Graphene Nanoplatelets, offers a robust strategy to mitigate degradation by enhancing interfacial adhesion and providing environmental insulation. Research shows that optimal weight percentages of these nanofillers can lead to a marked shift from adhesive to cohesive failure modes, even after prolonged aging.
- Modeling Fidelity: Cohesive Zone Modeling (CZM) has emerged as a powerful tool for predicting joint integrity. However, the accuracy of these models relies heavily on the empirical determination of environment-dependent Traction-Separation Laws (TSLs) that account for variables like strain rate, humidity, and temperature.

While accelerated aging methods like the open-face approach provide time-efficient data, significant challenges remain in correlating these results with the real-scale, long-term performance of joints.

While significant progress has been made in understanding joint degradation, a high-quality predictive framework requires transitioning from descriptive models to proactive, real-time assessments. Future research should prioritize the formulation of advanced Environment-dependent CZM approaches coupled with Physics-informed machine learning (PIML). Such hybrid algorithms have the potential to dynamically predict the non-linear degradation kinetics of nano-engineered adhesives under fluctuating hygrothermal conditions, significantly reducing the reliance on computationally expensive and time-consuming experimental aging tests. Furthermore, integrating these multi-scale predictive models into Digital Twins represents a critical frontier. By synergizing theoretical degradation models with data acquired through real-time structural health monitoring (SHM) sensors embedded within the bondline, engineers will be able to continuously assess the residual strength and predict the remaining fatigue life of bonded composite structures in service. This holistic, data-driven framework will be indispensable for the safe, reliable, and widespread implementation of multi-material adhesive joints in next-generation aerospace and automotive applications.

[Downloaded from rds.iust.ac.ir on 2026-11-19]

[DOI: 10.22068/ase.2026.741]

6. References

[1] Gibson RF. Principles of composite material mechanics: CRC press; 2007.

[2] Gheibi M, Shojaeefard M, Saeidi Googarchin H. Direct determination of a new mode-dependent cohesive zone model to simulate metal-to-metal adhesive joints. The Journal of Adhesion. 2019;95(10):943-70.

[3] Zaeri AR, Googarchin HS. Experimental investigation on environmental degradation of automotive mixed-adhesive joints. International Journal of Adhesion and Adhesives. 2019;89:19-29.

[4] Ghasempoor H, Keshavarzi A, Saeidi Googarchin H. Machine learning-enhanced prediction of energy absorption in AL/CFRP hybrid tubes under oblique compression. Mechanics of Advanced Materials and Structures. 2026 Dec 31;33(1):2627539.

[5] Phani KK, Bose NR. Hydrothermal ageing of CSM-laminate during water immersion—an acousto-ultrasonic study. Journal of Materials Science. 1986;21:3633-7.

[6] Da Silva LFM, Campilho RD, da Silva LF, Campilho RD. Advances in numerical modelling of adhesive joints: Springer; 2012.

[7] Budhe S, Banea M, de Barros S, Da Silva L. An updated review of adhesively bonded joints in composite materials. International journal of adhesion and adhesives. 2017;72:30-42.

[8] Ahmadi Z. Nanostructured epoxy adhesives: A review. Progress in Organic Coatings. 2019;135:449-53.

[9] Gheibi M, Shojaeefard M, Googarchin HS. Experimental and numerical analysis on the cohesive behavior of an automotive adhesive improved by MWCNT subjected to mode I and II loadings. International Journal of Mechanical Sciences. 2019;153:271-86.

[10] Mára V, Michalcová L, Kadlec M, Krčil J, Špatenka P. The effect of long-time moisture exposure and low temperatures on mechanical behavior of open-hole Cfrp laminate. Polymer Composites. 2021;42(7):3603-18.

[11] Aceti P, Carminati L, Bettini P, Sala G. Hygrothermal ageing of composite structures. Part 1: technical review. Composite Structures. 2023;319:117076.

[12] Golivari H, Googarchin HS, Zaeri A, Keshavarzi A. Experimental and numerical investigation of the energy absorption in hybrid double-hat thin-walled structures reinforced by adhesive bonding under three-point bending. International Journal of Adhesion and Adhesives. 2024;128:103543.

[13] Devin AB, Keshavarzi A, Googarchin HS. Harnessing predictable failure: a bio-inspired adhesively bonded Al/CFRP hybrid structure with guided crushing for enhanced crashworthiness under oblique loading. Materials & Design. 2026 Jan 7:115461.

[14] GhasemiPourMasoule SH, Keshavarzi A, Googarchin HS. A review on structural and mechanical insights into electric vehicle battery packs: Subsystems, standards, and design innovations. Journal of Energy Storage. 2026 May 15;158:121657.

[15] Zaeri AR, Saeidi Googarchin H. Analysis of automotive mixed-adhesive joints weakened by moist conditions: Experimental characterization and numerical simulation using cohesive zone model. Fatigue & Fracture of Engineering Materials & Structures. 2019;42(4):929-42.

[16] Keshavarzi A, Googarchin HS. Local reinforcement of adhesively bonded square shape aluminum energy absorber with CFRP under quasi-static axial loading: an experimental and numerical study. International Journal of Adhesion and Adhesives. 2024 Sep 5:103835.

[17] Ghasempoor H, Saeidi GH, Keshavarzi A. Finite element analysis of an adhesively bonded AlCFRP square section under axial & oblique loading. 2023.

[18] Attaf B. Ecobonding of composite wind turbine blade structural parts using eco-friendly adhesives. Adv Mater Sci Appl(AMSA). 2013;3:31-7.

[19] Khezri M, Keshavarzi A, Rooygari M, Googarchin HS, Shojaeefard MH. Designing High-Toughness Dissimilar Material Interfaces: A Bio-Inspired Fractal Approach to Laser Surface Engineering of Al/CFRP Joints. Composites Part C: Open Access. 2026 May 14:100744.

[20] Keshavarzi A, GhasemiPourMasoule SH, Googarchin HS. Synergistic toughening of dissimilar Al/CFRP adhesive joints via ternary Co-Zn-Al layered double hydroxides nanoparticles: Fracture mechanics and cohesive zone modeling. Materials & Design. 2026 Feb 14:115654.

[21] www.Nano.ir

[Downloaded from rds.iust.ac.ir on 2026-11-19]

[DOI: 10.22068/ase.2026.741]

[22] Špitalský Z, Kromka A, Matějka L, Černoch P, Kovářová J, Kotek J, et al. Effect of nanodiamond particles on properties of epoxy composites. Advanced composites letters. 2008;17(1):096369350801700104.

[23] Mochalin VN, Neitzel I, Etzold BJ, Peterson A, Palmese G, Gogotsi Y. Covalent incorporation of aminated nanodiamond into an epoxy polymer network. ACS nano. 2011;5(9):7494-502.

[24] Aris A, Shojaei A, Bagheri R. Cure kinetics of nanodiamond-filled epoxy resin: influence of nanodiamond surface functionality. Industrial & engineering chemistry research. 2015;54(36):8954-62.

[25] Haleem YA, Song P, Liu D, Wang C, Gan W, Saleem MF, et al. The effect of high concentration and small size of nanodiamonds on the strength of interface and fracture properties in epoxy nanocomposite. Materials. 2016;9(7):507.

[26] Hsiao K-T, Alms J, Advani SG. Use of epoxy/multiwalled carbon nanotubes as adhesives to join graphite fibre reinforced polymer composites. Nanotechnology. 2003;14(7):791.

[27] Yu S, Tong MN, Critchlow G. Wedge test of carbon-nanotube-reinforced epoxy adhesive joints. Journal of Applied Polymer Science. 2009;111(6):2957-62.

[28] Sung P-C, Chiu T-H, Chang S-C. Microwave curing of carbon nanotube/epoxy adhesives. Composites science and technology. 2014;104:97-103.

[29] Prolongo S, Gude M, Sanchez J, Ureña A. Nanoreinforced epoxy adhesives for aerospace industry. The Journal of Adhesion. 2009;85(4-5):180-99.

[30] Hickman G, Wallace LF, Burks VA, Hsiao K-T. Effects of carbon nanofiber reinforcments in adhesive bonding of cfrp. Soc Adv Mater Process Eng. 2012;11:35-50.

[31] Guadagno L, Sarno M, Vietri U, Raimondo M, Cirillo C, Ciambelli P. Graphene-based structural adhesive to enhance adhesion performance. RSC Advances. 2015;5(35):27874-86.

[32] Jia Z, Feng X, Zou Y. Graphene reinforced epoxy adhesive for fracture resistance. Composites Part B: Engineering. 2018;155:457-62.

[33] Vinod S, Tiwary CS, Samanta A, Ozden S, Narayanan TN, Vajtai R, et al. Graphene Oxide Epoxy (GO-xy): GO as Epoxy Adhesive by Interfacial Reaction of Functionalities. Advanced Materials Interfaces. 2018;5(2):1700657.

[34] Aradhana R, Mohanty S, Nayak SK. High performance electrically conductive epoxy/reduced graphene oxide adhesives for electronics packaging applications. Journal of Materials Science: Materials in Electronics. 2019;30:4296-309.

[35] Hu G, Zhang X, Liu L, Weng L. Improvement of graphene oxide/epoxy resin adhesive properties through interface modification. High Performance Polymers. 2019;31(3):341-9.

[36] Khalili SM, Tavakolian M, Sarabi A. Mechanical properties of nanoclay reinforced epoxy adhesive bonded joints made with composite materials. Journal of adhesion science and technology. 2010;24(11-12):1917-28.

[37] Aboubakr SH, Kandil UF, Taha MR. Creep of epoxy–clay nanocomposite adhesive at the FRP interface: A multi-scale investigation. International journal of adhesion and adhesives. 2014;54:1-12.

[38] Jouyandeh M, Jazani OM, Navarchian AH, Shabanian M, Vahabi H, Saeb MR. Bushy-surface hybrid nanoparticles for developing epoxy superadhesives. Applied Surface Science. 2019;479:1148-60.

[39] Srivastava S, Pandey A. Mechanical behavior and thermal stability of ultrasonically synthesized halloysite-epoxy composite. Composites Communications. 2019;11:39-44.

[40] Demir B, Chan K-Y, Yang D, Mouritz A, Lin H, Jia B, et al. Epoxy-gold nanoparticle nanocomposites with enhanced thermo-mechanical properties: An integrated modelling and experimental study. Composites Science and Technology. 2019;174:106-16.

[41] Tee D, Mariatti M, See C, Chong K, editors. Study on the electrical property of silver (Ag) nanoparticles filled epoxy composites for the application of electrically conductive adhesives (ECAs) in electronic packaging. 2006 Thirty-First IEEE/CPMT International Electronics Manufacturing Technology Symposium; 2006: IEEE.

[42] Dorigato A, Pegoretti A. The role of alumina nanoparticles in epoxy adhesives. Journal of Nanoparticle Research. 2011;13:2429-41.

[Downloaded from rds.iust.ac.ir on 2026-11-19]

[DOI: 10.22068/ase.2026.741]

[43] Jouyandeh M, Moini Jazani O, Navarchian AH, Saeb MR. High-performance epoxy-based adhesives reinforced with alumina and silica for carbon fiber composite/steel bonded joints. Journal of Reinforced Plastics and Composites. 2016;35(23):1685-95.

[44] Figueroa-Lara JdJ, Torres-Rodríguez M, Gutiérrez-Arzaluz M, Romero-Romo M. Effect of zirconia nanoparticles in epoxy-silica hybrid adhesives to join aluminum substrates. materials. 2017;10(10):1135.

[45] Ameer N. Effect of ZrO2 on Mechanical Strength, Antibacterial, and Anti Fungal of Epoxy Adhesive. Indian Journal of Natural Sciences. 2019;9(53).

[46] Bahlakeh G, Ghaffari M, Saeb MR, Ramezanzadeh B, De Proft F, Terryn H. A close-up of the effect of iron oxide type on the interfacial interaction between epoxy and carbon steel: combined molecular dynamics simulations and quantum mechanics. The Journal of Physical Chemistry C. 2016;120(20):11014-26.

[47] Zhao B, Hardiman M, Ryan KM, O'Reilly E, McCarthy C. Formation of reworkable nanocomposite adhesives by dielectric heating of epoxy resin embedded Fe 3 O 4 hollow spheres. CrystEngComm. 2016;18(32):6096-101.

[48] Imanaka M, Takeuchi Y, Nakamura Y, Nishimura A, Iida T. Fracture toughness of spherical silica-filled epoxy adhesives. International journal of adhesion and adhesives. 2001;21(5):389-96.

[49] Zhou H, Liu H-Y, Zhou H, Zhang Y, Gao X, Mai Y-W. On adhesive properties of nano-silica/epoxy bonded single-lap joints. Materials & Design. 2016;95:212-8.

[50] Ma J, Mo MS, Du XS, Dai SR, Luck I. Study of epoxy toughened by in situ formed rubber nanoparticles. Journal of Applied Polymer Science. 2008;110(1):304-12.

[51] Dugdale DS. Yielding of steel sheets containing slits. Journal of the Mechanics and Physics of Solids. 1960;8(2):100-4.

[52] Barenblatt GI. The mathematical theory of equilibrium cracks in brittle fracture. Advances in applied mechanics. 1962;7:55-129.

[53] Cornec A, Schönfeld W, Schwalbe K-H, Scheider I. Application of the cohesive model for predicting the residual strength of a large scale fuselage structure with a two-bay crack. Engineering failure analysis. 2009;16(8):2541-58.

[54] Du L, Wang Z, Gu T. A coupled thermo-mechanical cohesive zone model for strain rate-dependent fracture of hat-shaped specimens under impact. Engineering Fracture Mechanics. 2023;289:109382.

[55] Stigh U, Alfredsson KS, Andersson T, Biel A, Carlberger T, Salomonsson K. Some aspects of cohesive models and modelling with special application to strength of adhesive layers. International Journal of Fracture. 2010;165:149-62.

[56] Stone M, Peet T. Evaluation of the wedge cleavage test for assessment of durability of adhesive bonded joints. 1980.

[57] Rocha R, Campilho R. Evaluation of different modelling conditions in the cohesive zone analysis of single-lap bonded joints. The Journal of Adhesion. 2018;94(7):562-82.

[58] Wang W, Fernandes RL, De Freitas ST, Zarouchas D, Benedictus R. How pure mode I can be obtained in bi-material bonded DCB joints: a longitudinal strain-based criterion. Composites Part B: Engineering. 2018;153:137-48.

[59] Lißner M, Erice B, Alabort E, Thomson D, Cui H, Kaboglu C, et al. Multi-material adhesively bonded structures: Characterisation and modelling of their rate-dependent performance. Composites Part B: Engineering. 2020;195:108077.

[60] Hopfenberg H, Frisch H. Transport of organic micromolecules in amorphous polymers. Journal of Polymer Science Part B: Polymer Letters. 1969;7(6):405-9.

[61] Loh W, Crocombe A, Wahab MA, Ashcroft I. Environmental degradation of the interfacial fracture energy in an adhesively bonded joint. Engineering fracture mechanics. 2002;69(18):2113-28.

[62] Chang T, Sproat EA, Lai Y-H, Shephard NE, Dillard DA. A test method for accelerated humidity conditioning and estimation of adhesive bond durability. The Journal of Adhesion. 1997;60(1-4):153-62.

[63] Phani KK, Bose NR. Temperature dependence of hydrothermal ageing of CSM-laminate during water immersion. Composites science and technology. 1987;29(2):79-87.

[Downloaded from rds.iust.ac.ir on 2026-11-19]

[DOI: 10.22068/ase.2026.741]

[64] Nguyen T-C, Bai Y, Zhao X-L, Al-Mahaidi R. Durability of steel/CFRP double strap joints exposed to sea water, cyclic temperature and humidity. Composite structures. 2012;94(5):1834-45.

[65] Liljedahl C, Crocombe A, Wahab MA, Ashcroft I. Modelling the environmental degradation of the interface in adhesively bonded joints using a cohesive zone approach. The Journal of Adhesion. 2006;82(11):1061-89.

[66] Hua Y, Crocombe A, Wahab M, Ashcroft I. Continuum damage modelling of environmental degradation in joints bonded with EA9321 epoxy adhesive. International Journal of Adhesion and Adhesives. 2008;28(6):302-13.

[67] Loh W, Crocombe A, Wahab MA, Ashcroft I. Modelling anomalous moisture uptake, swelling and thermal characteristics of a rubber toughened epoxy adhesive. International journal of adhesion and adhesives. 2005;25(1):1-12.

[68] Han X, Crocombe A, Anwar S, Hu P, Li W. The effect of a hot–wet environment on adhesively bonded joints under a sustained load. The Journal of Adhesion. 2014;90(5-6):420-36.

[69] Crocombe A. Durability modelling concepts and tools for the cohesive environmental degradation of bonded structures. International journal of adhesion and adhesives. 1997;17(3):229-38.

[70] Goglio L, Rezaei M, Rossetto M. Moisture degradation of open-faced single lap joints. Journal of Adhesion Science and Technology. 2014;28(14-15):1382-93.

[71] Wylde J, Spelt J. Measurement of adhesive joint fracture properties as a function of environmental degradation. International Journal of Adhesion and Adhesives. 1998;18(4):237-46.

[72] Ameli A, Datla N, Papini M, Spelt J. Hygrothermal properties of highly toughened epoxy adhesives. The Journal of Adhesion. 2010;86(7):698-725.

[73] Heshmati M, Haghani R, Al-Emrani M. Durability of bonded FRP-to-steel joints: Effects of moisture, de-icing salt solution, temperature and FRP type. Composites Part B: Engineering. 2017;119:153-67.

[74] Liu S, Cheng X, Zhang Q, Zhang J, Bao J, Guo X. An investigation of hygrothermal effects on adhesive materials and double lap shear joints of CFRP composite laminates. Composites Part B: Engineering. 2016;91:431-40.

[75] Moidu AK, Sinclair AN, Spelt JK. Adhesive joint durability assessed using open-faced peel specimens. The Journal of Adhesion. 1998;65(1-4):239-57.

[76] Markatos D, Tserpes K, Rau E, Brune K, Pantelakis S. Degradation of mode-I fracture toughness of CFRP bonded joints due to release agent and moisture pre-bond contamination. The Journal of Adhesion. 2014;90(2):156-73.

[77] Park K, Paulino GH. Cohesive zone models: a critical review of traction-separation relationships across fracture surfaces. Applied Mechanics Reviews. 2011;64(6):060802.

[78] Carlberger T, Stigh U. Dynamic testing and simulation of hybrid joined bi-material beam. Thin-walled structures. 2010;48(8):609-19.

[79] May M, Hesebeck O, Marzi S, Böhme W, Lienhard J, Kilchert S, et al. Rate dependent behavior of crash-optimized adhesives–Experimental characterization, model development, and simulation. Engineering Fracture Mechanics. 2015;133:112-37.

[80] Gheibi M, Shojaeefard M, Googarchin HS. A comparative study on the fracture energy determination theories for an automotive structural adhesive: Experimental and numerical investigation. Engineering Fracture Mechanics. 2019;212:13-27.

[81] Peres L, Arnaud M, Silva A, Campilho R, Machado J, Marques E, et al. Geometry and adhesive optimization of single-lap adhesive joints under impact. The Journal of Adhesion. 2022;98(6):677-703.

[82] Liljedahl C, Crocombe A, Wahab M, Ashcroft I. Modelling the environmental degradation of adhesively bonded aluminium and composite joints using a CZM approach. International Journal of Adhesion and Adhesives. 2007;27(6):505-18.

[83] Costa M, Viana G, Créac'Hcadec R, Da Silva L, Campilho R. A cohesive zone element for mode I modelling of adhesives degraded by humidity and fatigue. International Journal of Fatigue. 2018;112:173-82.

[84] Machado J, Hayashi A, Sekigushi Y, Campilho R, Marques E, Sato C, et al. Dynamic behaviour in mode I fracture toughness of CFRP as a function of temperature. Theoretical and Applied Fracture Mechanics. 2019;103:102257.

[Downloaded from rds.iust.ac.ir on 2026-11-19]

[DOI: 10.22068/ase.2026.741]

[85] Li Y, Yang Y, Li J, Wang B, Liao Y. Experimental-numerical analysis of failure of adhesively bonded lap joints under transverse impact and different temperatures. International Journal of Impact Engineering. 2020;140:103541.

[86] Johar M, Wong K, Rashidi S, Tamin M. Effect of strain-rate and moisture content on the mechanical properties of adhesively bonded joints. Journal of Mechanical Science and Technology. 2020;34:1837-45.

[87] Marzi S, Hesebeck O, Brede M, Kleiner F, editors. A rate-dependent, elasto-plastic cohesive zone mixed-mode model for crash analysis of adhesively bonded joints. 7th European LS-DYNA conference; 2009.

[88] Valente J, Campilho R, Marques E, Machado J, Da Silva L. Adhesive joint analysis under tensile impact loads by cohesive zone modelling. Composite Structures. 2019;222:110894.

[89] Lissner M, Alabort E, Cui H, Rito R, Blackman B, Petrinic N. Experimental characterisation and numerical modelling of the influence of bondline thickness, loading rate, and deformation mode on the response of ductile adhesive interfaces. Journal of the Mechanics and Physics of Solids. 2019;130:349-69.

[90] Machado J, Nunes P, Marques E, Campilho R, da Silva LF. Numerical study of mode I fracture toughness of carbon-fibre-reinforced plastic under an impact load. Proceedings of the Institution of Mechanical Engineers, Part L: Journal of Materials: Design and Applications. 2020;234(1):12-20.

[91] Carbas R, Da Silva L, Marques E, Lopes A. Effect of post-cure on the glass transition temperature and mechanical properties of epoxy adhesives. Journal of Adhesion Science and Technology. 2013;27(23):2542-57.

[92] Zhang Y, Adams R, da Silva LF. Effects of curing cycle and thermal history on the glass transition temperature of adhesives. The Journal of Adhesion. 2014;90(4):327-45.

[93] Bauwens JC. Relation between the compression yield stress and the mechanical loss peak of bisphenol-A-polycarbonate in the β transition range. Journal of Materials Science. 1972;7:577-84.

[94] Bauwens-Crowet C, Bauwens J-C, Homes G. The temperature dependence of yield of polycarbonate in uniaxial compression and tensile tests. Journal of Materials Science. 1972;7:176-83.

[95] Banea M, Da Silva L, Campilho R. Mode I fracture toughness of adhesively bonded joints as a function of temperature: experimental and numerical study. International Journal of Adhesion and Adhesives. 2011;31(5):273-9.

[96] Blackman B, Kinloch A, Taylor A, Wang Y. The impact wedge-peel performance of structural adhesives. Journal of materials science. 2000;35:1867-84.

[97] Adamvalli M, Parameswaran V. Dynamic strength of adhesive single lap joints at high temperature. International Journal of Adhesion and Adhesives. 2008;28(6):321-7.

[98] Carlberger T, Biel A, Stigh U. Influence of temperature and strain rate on cohesive properties of a structural epoxy adhesive. International Journal of Fracture. 2009;155:155-66.

[99] Machado J, Marques E, Campilho R, da Silva LF. Mode I fracture toughness of CFRP as a function of temperature and strain rate. Journal of Composite Materials. 2017;51(23):3315-26.

[100] Gledhill R, Kinloch A. Environmental failure of structural adhesive joints. The journal of adhesion. 1974;6(4):315-30.

[101] Pethrick RA. Design and ageing of adhesives for structural adhesive bonding–a review. Proceedings of the Institution of Mechanical Engineers, Part L: Journal of Materials: design and applications. 2015;229(5):349-79.

[102] Kinloch A, Little M, Watts J. The role of the interphase in the environmental failure of adhesive joints. Acta materialia. 2000;48(18-19):4543-53.

[103] ASHCROFT I. The effect of residual strains on the progressive damage modelling of environmentally degraded adhesive joints.

[104] Moazzami M, Ayatollahi M, Akhavan-Safar A, Da Silva L. Experimental and numerical analysis of cyclic aging in an epoxy-based adhesive. Polymer Testing. 2020;91:106789.

[105] Budhe S, Banea M, de Barros S. Bonded repair of composite structures in aerospace application: a review on environmental issues. Applied Adhesion Science. 2018;6:1-27.

[106] Viana G, Costa M, Banea M, da Silva LF. Water diffusion in double cantilever beam adhesive joints.

[Downloaded from rds.iust.ac.ir on 2026-11-19]

[DOI: 10.22068/ase.2026.741]

Latin American Journal of Solids and Structures. 2017;14:188-201.

[107] Pérez-Pacheco E, Cauich-Cupul J, Valadez-González A, Herrera-Franco P. Effect of moisture absorption on the mechanical behavior of carbon fiber/epoxy matrix composites. Journal of materials science. 2013;48:1873-82.

[108] Jiang X, Qiang X, Kolstein M, Bijlaard F, editors. Experimental Study on Mechanical Behaviour of FRP-to-steel Adhesively-bonded Joints after Hygrothermal Aging. IABSE Symposium: Engineering for Progress, Nature and People, Madrid, Spain, 3-5 September 2014; 2014.

[109] Mariam M, Afendi M, Majid MA, Ridzuan M, Azmi A, Sultan M. Influence of hydrothermal ageing on the mechanical properties of an adhesively bonded joint with different adherends. Composites Part B: Engineering. 2019;165:572-85.

[110] Moazzami M, Ayatollahi M, Akhavan-Safar A, De Freitas ST, Poulis J, da Silva L. Effect of cyclic aging on mode I fracture energy of dissimilar metal/composite DCB adhesive joints. Engineering Fracture Mechanics. 2022;271:108675.

[111] Yu Y, Jia X, Han X, Ding G, Hou W. Analytical investigation of hygrothermal effects on failure mechanisms of adhesively bonded corrugated sandwich structures under three-point bending. International Journal of Adhesion and Adhesives. 2024;128:103561.

[112] Abdel-Monsef S, Renart J, Carreras L, Maimí P, Turon A. Environmental effects on the cohesive laws of the composite bonded joints. Composites Part A: Applied Science and Manufacturing. 2022;155:106798.

[113] Gkikas G, Lekatou A, Sioulas D, Paipetis A. Effect of carbon nanotube enhanced adhesives on degradation of bonded joints in corrosive environments. Plastics, Rubber and Composites. 2014;43(10):322-9.

[114] Khoramishad H, Ashofteh R, Mobasheri M, Berto F. Temperature dependence of the shear strength in adhesively bonded joints reinforced with multi-walled carbon nanotubes. Engineering Fracture Mechanics. 2018;199:179-87.

[115] Hajizamani E, Jazani OM, Riazi H. Design and characterization of a novel supported epoxy film adhesive reinforced by Ti3C2Tx MXene nanoparticles. Materials Chemistry and Physics. 2023;308:128270.

[116] Esmail R, Alaei MH, Eskandarijam J, Rezvaninasab M. Effect of presence of SWCNT and Fullerene nano particles in the adhesive of CFRP single lap joint on the lap shear strength subjected to hygrothermal conditions. Journal of Adhesion Science and Technology. 2023;37(21):3013-29.

[117] Farzanehfar N, Taheri A, Rafiemanzelat F, Jazani OM. High-performance epoxy nanocomposite adhesives with enhanced mechanical, thermal and adhesion properties based on new nanoscale ionic materials. Chemical Engineering Journal. 2023;471:144428.

[118] Ceylan R, Ozun E, Çoban O, Bora MÖ, Kutluk T. The effect of hygrothermal aging on the adhesion performance of nanomaterial reinforced aluminium adhesive joints. International Journal of Adhesion and Adhesives. 2023;121:103304.

[119] Ejaz H, Mubashar A, Uddin E, Ali Z. A comparative study of GNPs and MWCNTs additives on dispersion behavior and strength characteristics of the adhesively bonded joints. Journal of Dispersion Science and Technology. 2024;45(2):272-83.

[120] Aradhana R, Mohanty S, Nayak SK. High performance epoxy nanocomposite adhesive: Effect of nanofillers on adhesive strength, curing and degradation kinetics. International Journal of Adhesion and Adhesives. 2018;84:238-49.

[121] Gilbert EN, Hayes BS, Seferis JC. Nano-alumina modified epoxy based film adhesives. Polymer Engineering & Science. 2003;43(5):1096-104.

[122] Gupta SK, Shukla DK, Bharti A, editors. Effect of alumina nanoparticles on shear strength of epoxy adhesive: experimental and finite element analysis. 2017 International Conference on Advances in Mechanical, Industrial, Automation and Management Systems (AMIAMS); 2017: IEEE.

[123] Jakubinek MB, Ashrafi B, Zhang Y, Martinez-Rubi Y, Kingston CT, Johnston A, et al. Single-walled carbon nanotube–epoxy composites for structural and conductive aerospace adhesives. Composites Part B: Engineering. 2015;69:87-93.

[124] Khoee S, Hassani N. Adhesion strength improvement of epoxy resin reinforced with nanoelastomeric copolymer. Materials Science and Engineering: A. 2010;527(24-25):6562-7.

[Downloaded from rds.iust.ac.ir on 2026-11-19]

[DOI: 10.22068/ase.2026.741]

[125] Jojibabu P, Jagannatham M, Haridoss P, Ram GJ, Deshpande AP, Bakshi SR. Effect of different carbon nano-fillers on rheological properties and lap shear strength of epoxy adhesive joints. Composites Part A: Applied Science and Manufacturing. 2016;82:53-64.

[126] Quan D, Carolan D, Rouge C, Murphy N, Ivankovic A. Carbon nanotubes and core–shell rubber nanoparticles modified structural epoxy adhesives. Journal of Materials Science. 2017;52:4493-508.

[127] Ma H-L, Jia Z, Lau K-t, Li X, Hui D, Shi S-q. Enhancement on mechanical strength of adhesively-bonded composite lap joints at cryogenic environment using coiled carbon nanotubes. Composites Part B: Engineering. 2017;110:396-401.

[128] Quan D, Carolan D, Rouge C, Murphy N, Ivankovic A. Mechanical and fracture properties of epoxy adhesives modified with graphene nanoplatelets and rubber particles. International Journal of Adhesion and Adhesives. 2018;81:21-9.

[129] Salom C, Prolongo M, Toribio A, Martínez-Martínez A, de Cárcer IA, Prolongo S. Mechanical properties and adhesive behavior of epoxy-graphene nanocomposites. International Journal of Adhesion and Adhesives. 2018;84:119-25.

[130] Ilyin S, Brantseva T, Gorbunova IY, Antonov S, Korolev YM, Kerber M. Epoxy reinforcement with silicate particles: Rheological and adhesive properties–Part I: Characterization of composites with natural and organically modified montmorillonites. International Journal of Adhesion and Adhesives. 2015;61:127-36.

[131] Lin W, Xi X, Yu C. Research of silver plating nano-graphite filled conductive adhesive. Synthetic Metals. 2009;159(7-8):619-24.

[132] Ghosh P, Kumar K, Preeti P, Rajoria M, Misra N. Superior dissimilar adhesive joint of mild steel and aluminium using UDM processed epoxy based TiO2 nano-filler composite adhesive. Composites Part B: Engineering. 2016;99:224-34.

[133] Dorigato A, Pegoretti A, Bondioli F, Messori M. Improving epoxy adhesives with zirconia nanoparticles. Composite Interfaces. 2010;17(9):873-92.

[134] Mansourian-Tabaei M, Jafari SH, Khonakdar HA. Lap shear strength and thermal stability of diglycidyl ether of bisphenol a/epoxy novolac adhesives with nanoreinforcing fillers. Journal of applied polymer science. 2014;131(6).

[Downloaded from rds.iust.ac.ir on 2026-11-19]

[DOI: 10.22068/ase.2026.741]